Magnesium alloys of the rare earth metals: systematics and properties

R. Ferro, A. Saccone and S. Delfino
Dipartimento di Chimica e Chimica Industriale, Università di Genova, Genova, Italy

Abstract

Recent literature data on the possible technological beneficial effects of the addition of rare earth metals (R) to magnesium based alloys are briefly reported.

The constitutional properties (crystallochemistry, thermodynamics, phase equilibria) of binary R-Mg alloys are reviewed, subdividing the different groups of systems as the following: those given by the light R, those formed by the heavy R (to which yttrium has to be added) and by scandium and finally the systems with the "divalent" rare earths, europium and ytterbium (which show a number of analogies with the typical divalent alkaline earth metals).

Properties and characteristics of the Mg-rich alloys are especially described and discussed (Mg solid solutions, stoichiometries and structures, stable and metastable equilibria corresponding to the Mg-richest phases).

Several properties of R-Mg alloys change smoothly as a function of the atomic dimension of the trivalent rare earth: similar dependence is also observed in ternary R'-R"-Mg alloys, formed by two different trivalent rare earth metals, for which the averaged radius of the R'-R" mixture involved may be used as the corresponding reference parameter. This allows a semi-quantitative check of the reliability of a given R-Mg system and can be used as a first criterion for predicting phase stoichiometries, crystallochemistry and properties of selected ternary alloys in order to design and plan their structures and characteristics.

Details are also given about peculiarities and problems in the experimental determination of phase equilibria and the thermodynamics of Mg alloys with the rare earth metals, with particular reference to the work carried out by the authors research group.

Riassunto

Sono descritti alcuni aspetti del comportamento in lega del magnesio con il gruppo di metalli delle "terre rare" (scandio, ittrio, lantanidi).

Sono brevemente richiamati gli effetti su alcune proprietà tecnologiche, di addizioni di terre rare al magnesio e ricordate le caratteristiche di tipiche leghe commerciali a base di magnesio contenenti aggiunte di questi metalli.

Sono presentati gli elementi per una descrizione sistematica delle leghe binarie del magnesio con i diversi metalli delle terre rare (in particolare di quelle trivalenti) evidenziando in particolare gli andamenti delle cosiddette proprietà costituzionali (cristallochimica, termodinamica, composizione, struttura ed equilibri di fase). Sono discusse le regolarità di andamenti di struttura e proprietà osservati per particolari gruppi di leghe quali quelle ad alto contenuto in magnesio.

Con riferimento, infine, anche al lavoro sperimentale condotto nel laboratorio degli autori, sono illustrati alcuni risultati ottenuti nella classificazione e predizione delle fasi e degli equilibri osservabili in leghe ternarie del magnesio contenenti due diversi metalli delle terre rare trivalenti.

PRELIMINARY REMARKS ON THE GENERAL PROPERTIES OF THE RARE EARTH METALS AND THEIR ALLOYING BEHAVIOUR

As an introduction to the alloying behaviour of the rare earth metals (R) with magnesium, it could be useful to remember the position of these elements in the Periodic Table and their typical atomic properties. Scandium (atomic number 21), yttrium (atomic number 39), lanthanum and lanthanides (atomic number from 57 to 72) all together form the group of the rare earth metals (see Fig.1). They can be subdivided into two groups: the so-called "light" rare earths from La to Eu and the "heavy" ones from Gd to Lu. Generally, yttrium is added to the latter because of the value of its atomic radius and its characteristic behaviour. Eu and Yb behave in a different way, usually being divalent instead of trivalent like the other rare earth metals. The electronic structure of the rare earth elements is summarised in Table 1, in which the data are given for the free gaseous atom (ground state configuration) for the typical R^{2+}, R^{3+} and R^{4+} ionic species and for the metallic form. The normal configuration for the metallic state is n electrons in the 4f orbitals and 3 electrons in the (5d + 6s) orbitals (trivalent state) with only Eu and Yb having a divalent configuration.

A few characteristic trends of some properties of the rare earth metals are highlighted, according to Gschneidner [1], in the following. The trend of the metallic radius of the lanthanides in function of their atomic number is shown in Fig.2.

TABLE 1 - Electronic structures of the rare earth metals in the ground state, in the metallic form and in their common states of oxidation

Element	Ground state Configuration		Metallic state Number of electrons		Ionic species 4f Configuration		
			Valence	4f	R^{2+}	R^{3+}	R^{4+}
Sc	–	$3d^1\ 4s^2$	3	0	–	0	–
Y	–	$4d^1\ 5s^2$	3	0	–	0	–
La	–	$5d^1\ 6s^2$	3	0	–	0	–
Ce	$4f^1$	$5d^1\ 6s^2$	3	1	–	1	0
Pr	$4f^3$	$6s^2$	3	2	–	2	1
Nd	$4f^4$	$6s^2$	3	3	–	3	–
Pm	$4f^5$	$6s^2$	3	4	–	4	–
Sm	$4f^6$	$6s^2$	3	5	6	5	–
Eu	$4f^7$	$6s^2$	2	7	7	6	–
Gd	$4f^7$	$5d^1\ 6s^2$	3	7	–	7	–
Tb	$4f^9$	$6s^2$	3	8	–	8	7
Dy	$4f^{10}$	$6s^2$	3	9	–	9	–
Ho	$4f^{11}$	$6s^2$	3	10	–	10	–
Er	$4f^{12}$	$6s^2$	3	11	–	11	–
Tm	$4f^{13}$	$6s^2$	3	12	–	12	–
Yb	$4f^{14}$	$6s^2$	2	14	14	13	–
Lu	$4f^{14}$	$5d^1\ 6s^2$	3	14	–	14	–

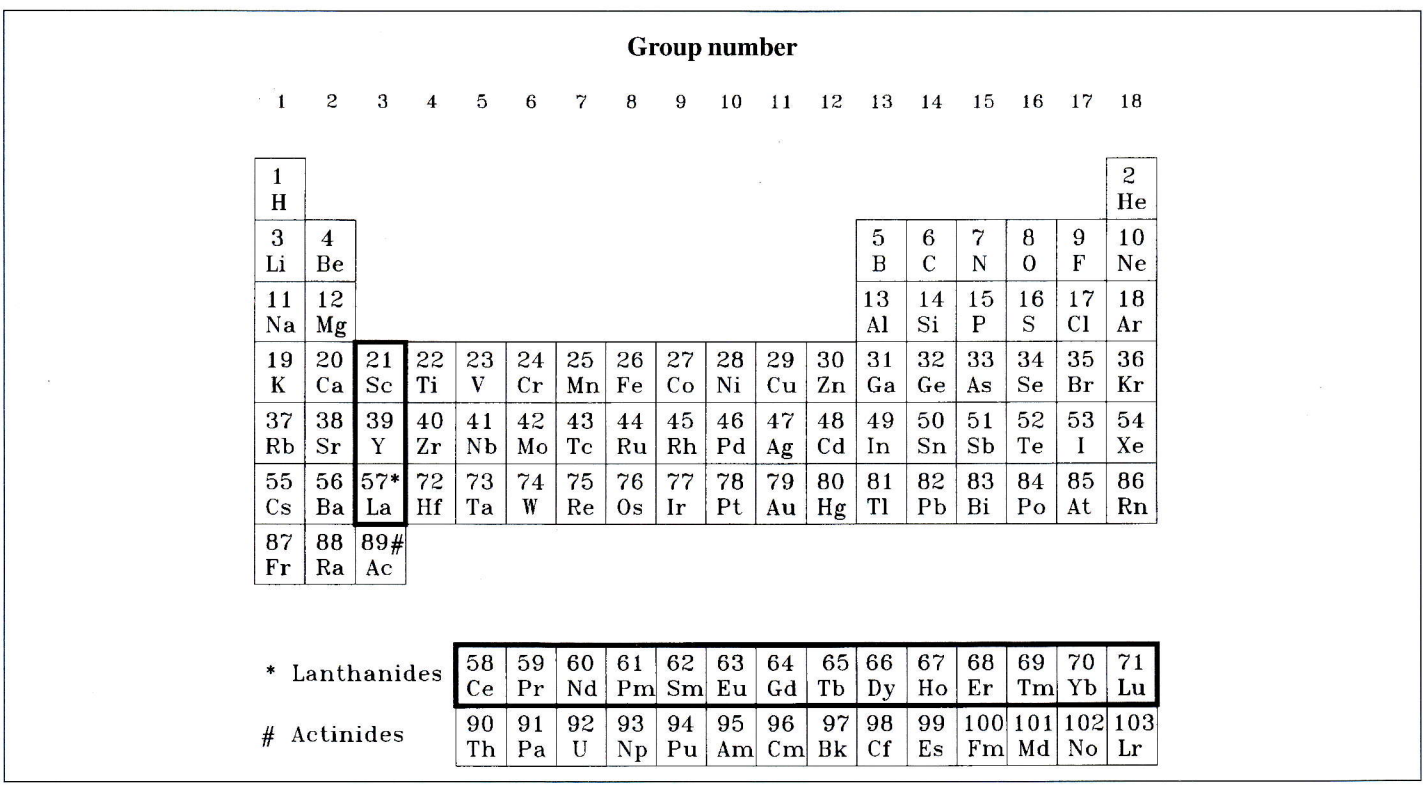

Figure 1: Periodic table of the elements. The different elements and their atomic number are shown; the rare earth metals are evidenced.

In this figure, the yttrium value has been inserted between the Dy and Ho radii according to the data reported by Teatum [2]. Notice, however, that, in the definition of the yttrium radius, different conventions can be considered resulting in a value very close either to that of Gd or Dy. The value of the Sc radius (164 pm, much smaller than the other rare earths) is not added. A large decrease in the atomic dimension of the trivalent rare earths is evident on passing from the light to heavy rare earths. This is commonly called "lanthanide contraction". Fig. 3 reports the lanthanide melting points and the transformation temperatures (from the close-packed face-centred cubic (fcc) (La, Ce), from the double c hexagonal close-packed (dhcp) (Pr, Nd, Pm) and from the hexagonal close-packed (hcp) (Sm, Gd, Tb, Dy) to the body-centered cubic (bcc) structures) versus their atomic number. Finally, the free energies (ΔG) of formation of the rare earth oxides are reported in Fig. 4, as an indication of the reactivity of such elements. A very high stability of the R oxides is noticed specially if it is compared with the oxides of other metals.

Fig. 2

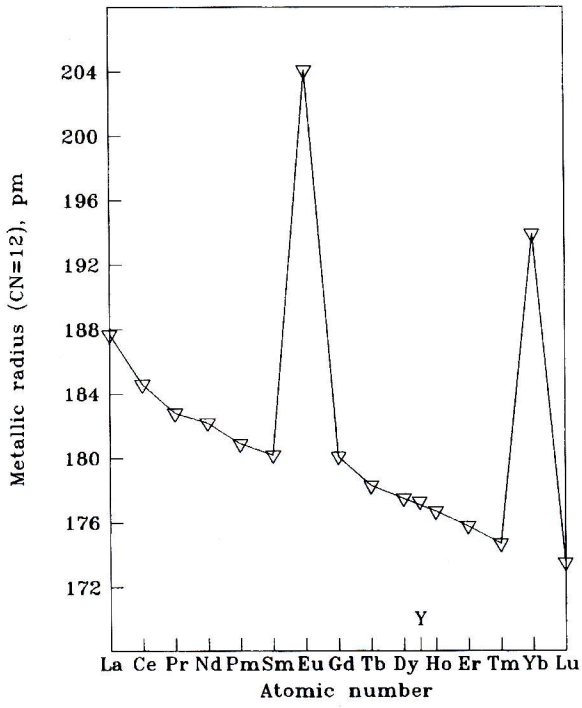

Fig. 3

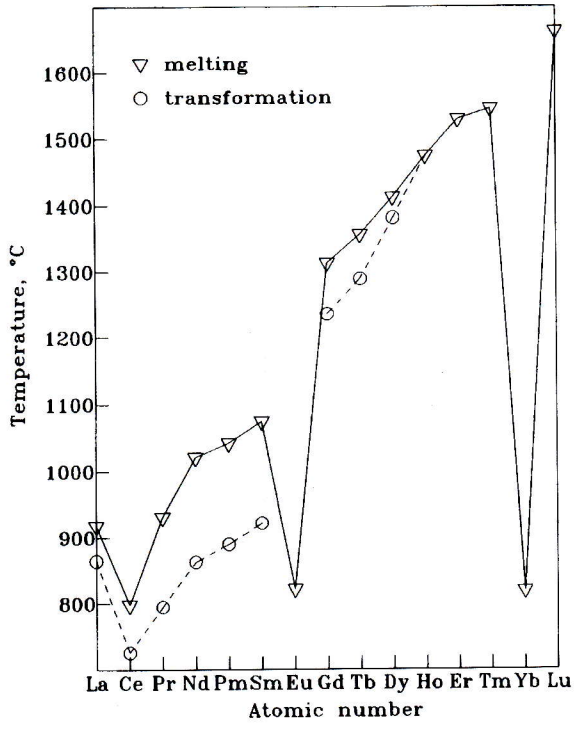

Figure 2: The metallic radius (coordination 12) of the lanthanides is reported against their atomic number. The yttrium value has been added

Figure 3: The melting and the highest solid state transformation (to the bcc form) temperatures of the lanthanides are reported versus their atomic number

The general alloying behaviour of the trivalent rare earth metals is summarised in Fig. 5, where it is reported for two typical rare earths, La, as a representative of the light trivalent rare earths and Gd, as representative of the heavy ones. This figure evidences the compound formation capability, that is, the number of compounds formed by the rare earth involved with the different elements identified according to their position in the Periodic Table. No compounds, besides Be and Mg, are formed with the elements on the left of the Periodic Chart. The phase diagrams, of the rare earths with these elements are generally very simple, in many cases of the eutectic type, and often show a miscibility gap also in the liquid state. Be and Mg are exceptions, giving more complex systems. On the contrary, the rare earth metals show very high reactivity with the elements on the right of the Periodic Chart, with which they form several compounds, in many cases presenting high melting temperatures and high heats of formation.

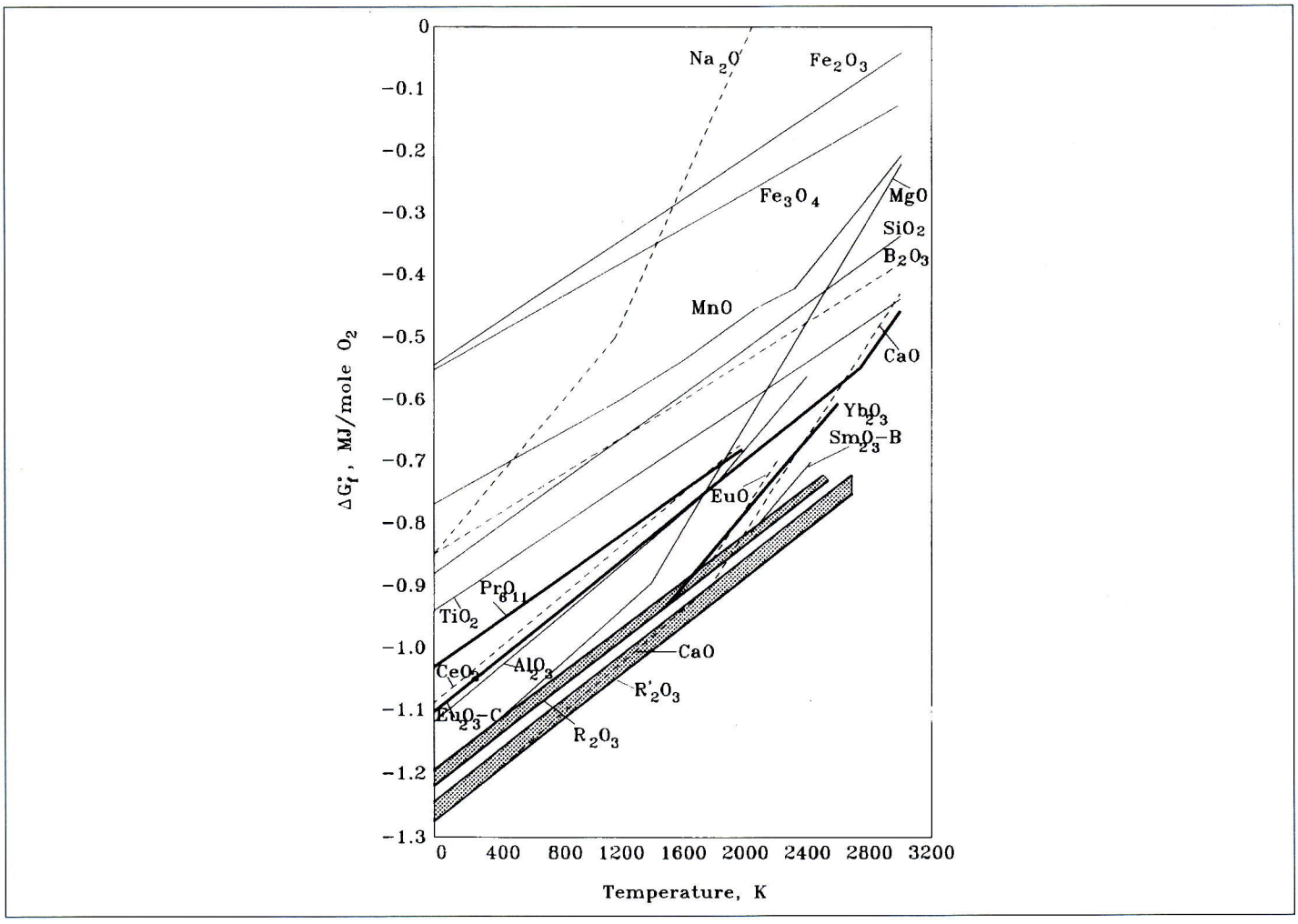

Figure 4: Standard free energies of formation of rare earth and selected non-rare earth oxides. The ranges of values of the free energies relevant to the light lanthanide metal sesquioxides (R_2O_3) and to the heavy lanthanide metal sesquioxides (R'_2O_3) are shown

COMMENTS ON THE EFFECT OF RARE EARTH ADDITIONS ON SELECTED TECHNOLOGICAL PROPERTIES OF Mg ALLOYS

On considering the Mg alloys of the rare earths, we may notice that the Mg-R systems are characterised by complex phase diagrams showing several compounds some of which often have very high Mg content. Specifically we see in Fig. 5 that with magnesium, represented in the Periodic Chart by the 2nd box in the 2nd column (compare with Fig. 1), lanthanum forms 6 compounds (two of which are very close in their compositions) and gadolinium 4. Details of the crystal structures and the phase diagrams of the Mg-R systems will be reported after a few comments about the effects of R additions on some technological properties of magnesium.
In the following a little information, taken from books such as "ASM Handbook" [1, 3] and "Structure and Properties of Nonferrous Alloys" [4], on commercial Mg-based rare earth alloys is outlined.

Preliminary remarks

The application of rare earths as alloy additives in metallurgy depends on one or more of the following properties:

- A high chemical affinity with elements such as carbon, nitrogen, oxygen, sulphur.
- Metallic size
- Low vapour pressure
- Alloy formation properties.

In many of these applications the rare earths are added as the naturally occurring mixture of elements as reduced from monazite or bastnasite ore. This material, having an approximate rare earth composition of 50% Ce, 30% La, 15% Nd and 5% Pr, is called Mischmetal (usually indicated as MM). Sometimes the addition of a mixture of rare-earth elements made up chiefly of Nd and Pr (for instance 80 Nd - 20Pr) is also considered. This mixture is also called didymium (Di or Dm).

See Tables 2 and 3 for a short summary (adapted from "ASM Handbook" [3]) of the codes used in the designation of these alloys and of typical properties of selected alloys.

As for the magnesium alloys we may underline that the alloy behaviour of this metal is notable for the variety of elements with which it forms solid solutions, including the rare earths. R-alloys developed early used mischmetal (MM) to reduce microporosity in wrought alloys such as Mg-1.25Zn-0.17MM. This alloy was difficult to cast, but other alloys containing various amounts of zinc, zirconium and mischmetal were developed with good castability. Rare earth additions are especially effective in improving the creep resistance of magnesium-base alloys. The rare earths also refine the grain size and improve the strength, ductility, toughness, weldability, machinability and corrosion resistance. Recently developed alloys have contained separate rare earths. Didymium (Nd-Pr mixture) is the most effective, followed by cerium-free mischmetal, mischmetal, cerium and lanthanum, in order of decreasing effectiveness.

A Mg-Al-Zn-Nd alloy has good corrosion resistance in an aqueous saline solution. Also a Mg-Y-Nd-Zr alloy was shown to have good corrosion resistance, good castability, and stability to 300°C.

TABLE 2 - Magnesium alloys: standard ASTM system of alloy (and temper) designation

First part

consists of two code letters representing the two main alloying elements arranged in order of decreasing percentage according to the following symbols:
A: aluminium; B: bismuth; C: copper; D: cadmium; E: rare earth; F: iron; G: magnesium; H: thorium; K: zirconium; L: lithium; M: manganese; N: nickel; P: lead; Q: silver; R: chromium; S: silicon; T: tin; W: yttrium; Y: antimony; Z: zinc

Second part

indicates the amounts of the two principal alloying elements by two digits corresponding to rounded-off percentages of these elements.

Third part

Distinguishes between different alloys with the same percentages of the two principal alloying elements and consists of a letter assigned in order as compositions become standard.

Fourth part

Indicates temper conditions according to the following symbols:
F: as fabricated; O: annealed; H10 and H11: slightly strain hardened; H23, H24 and H26: strain hardened and partially annealed; T4: solution heat treated; T5: artificially aged only; T6: solution heat treated and artificially aged; T8: solution heat treated, cold worked ad artificially aged.

Example: the alloy designated by AZ91E-T6 contains Al and Zn as principal alloying components. The rounded-off percentages of these elements are 9 and 1, respectively. The letter E specifies that this is the 5th alloy standardised with 9% Al and 1% Zn as principal additions. The T6 symbol indicates that this is a solution heat treated and artificially aged.

TABLE 3 - Selected examples of magnesium alloys with or without R elements are reported. Nominal compositions and typical room-temperature nechanical properties of sand and permanent mold casting alloys are presented

	Composition, mass %						Tensile Strength		Tensile		Yield strength Compressive		Bearing		Elongation in 50 mm (2 in)	Shear Strength		Hardness
Alloy	Al	Mn	Th	Zn	Zr	Other	MPa	ksi	Mpa	ksi	MPa	ksi	MPa	ksi	%	MPa	ksi	HRB
AM100A-T61	10.0	0.1	—	—	—	—	275	40	150	22	150	22	—	—	1	—	—	69
AZ63A-T6	6.0	0.15	—	3.0	—	—	275	40	130	19	130	19	360	52	5	145	21	73
AZ91C and AZ91E-T6	8.7	0.13	—	0.7	—	—	275	40	145	21	145	21	360	52	6	145	21	66
EQ21A-T6	—	—	—	—	0.7	1.5Ag 2.1Di	235	34	195	28	195	28	—	—	2	—	—	65-85
EZ33A-T5	—	—	—	2.7	0.6	3.3 R	160	23	110	16	110	16	275	40	2	145	21	50
QE22-T6	—	—	—	—	0.7	2.5 Ag 2.1 Di	260	38	195	28	195	28	—	—	3	—	—	80
QH21A-T6	—	—	1.0	—	0.7	2.5 Ag 1.0 Di	275	40	205	30	—	—	—	—	4	—	—	—
WE43A-T6	—	—	—	—	0.7	4.0 Y 3.4 R	250	36	165	24	—	—	—	—	2	—	—	75-95
WE54A-T6	—	—	—	—	0.7	5.2 Y 3.0 R	250	36	172	25	172	25	—	—	2	—	—	75-95
ZE41A-T5	—	—	—	4.2	0.7	1.2 R	205	30	140	20	140	20	350	51	3.5	160	23	62
ZE63A-T6	—	—	—	5.8	0.7	2.6 R	300	44	190	28	195	28	—	—	10	—	—	60-85
ZH62A-T5	—	—	1.8	5.7	0.7	—	240	35	170	25	170	25	340	49	4	165	24	70
ZK61A-T5	—	—	—	6.0	0.7	—	310	45	185	27	185	27	—	—	—	170	25	68

Mention of selected Mg alloys containing R and of their properties (According to refs. [3, 4])

As an example selected mechanical properties of some magnesium-rare earth alloys are reported in Figs. 6 and 7.

Sand and permanent mold casting alloys.

Several systems of magnesium alloys are available for sand and permanent mold castings:

- Magnesium-aluminium-manganese with and without zinc (AM and AZ)
- Magnesium-zirconium (K)
- Magnesium-zinc-zirconium with and without zinc (HK, HZ and ZH)
- Magnesium-silver-zirconium with rare earths or thorium (QE and QH)
- Magnesium-yttrium-rare earth-zirconium (WE)
- Magnesium-zinc-copper-manganese (ZC)

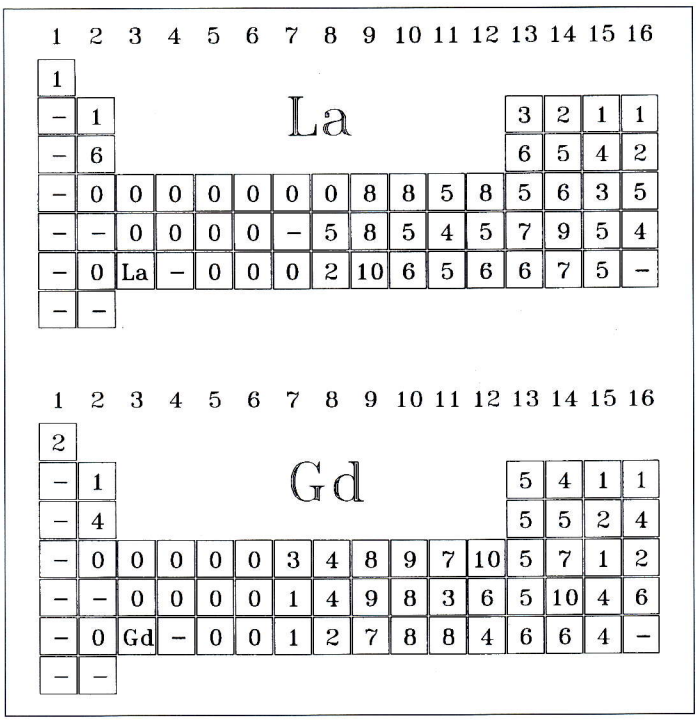

Figure 5: Compound formation capability of two typical lanthanides, La (light rare earth metal) and Gd (heavy rare earth metal). The number of intermediate phases formed with the different elements (represented by their position in the Periodic Table) is given. "0" means that the phase diagram has been studied and no compounds have been found; "-" means that the phase diagram has not been studied and no compounds have been identified

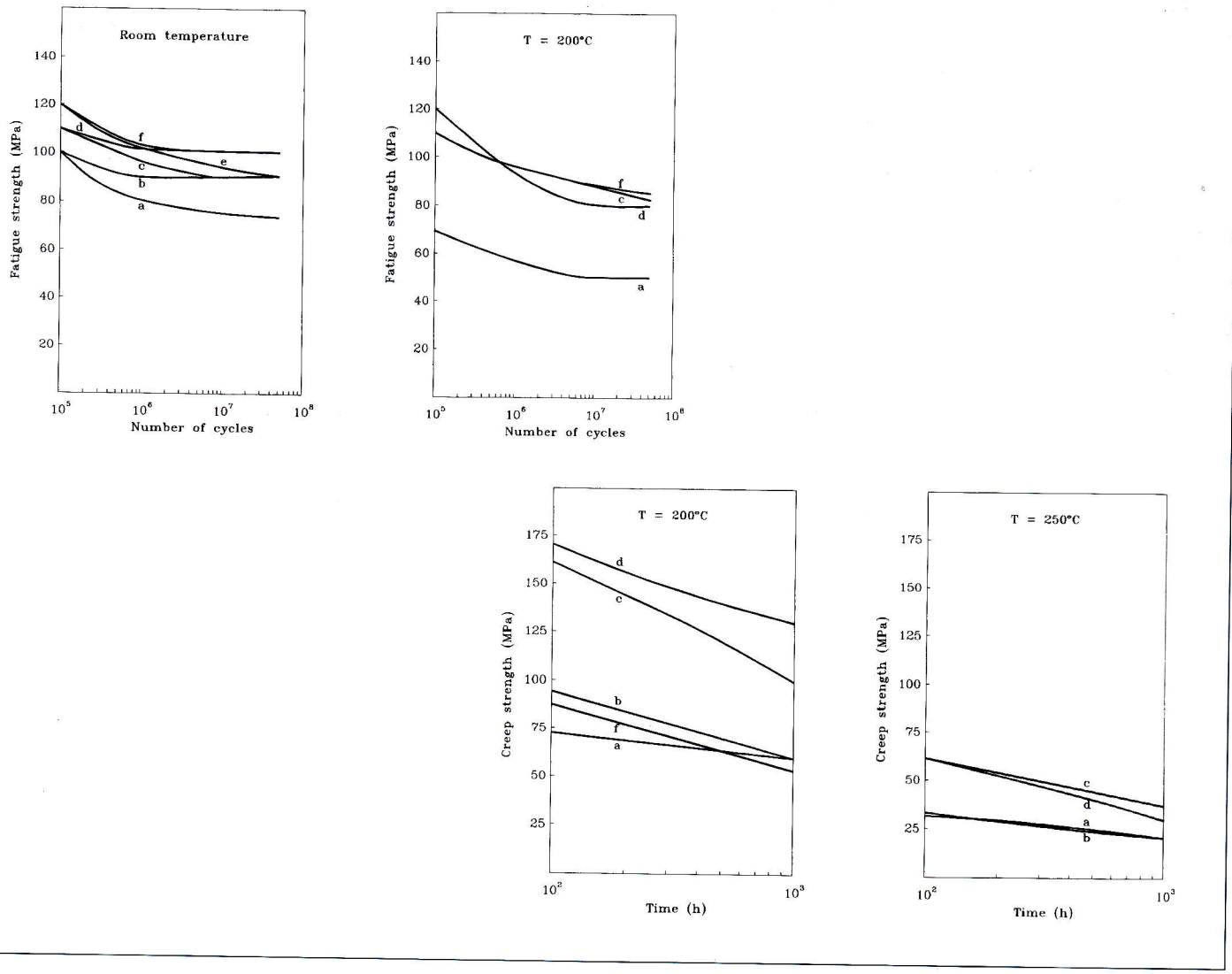

Figure 6: Fatigue strength (upper part of the figure) and creep strength (lower part) of some magnesium -rare earth alloys at different temperatures. (From ref. [4]). a: EZ33; b: EQ21; c: WE43; d: WE54; e: ZE41; f: QE22

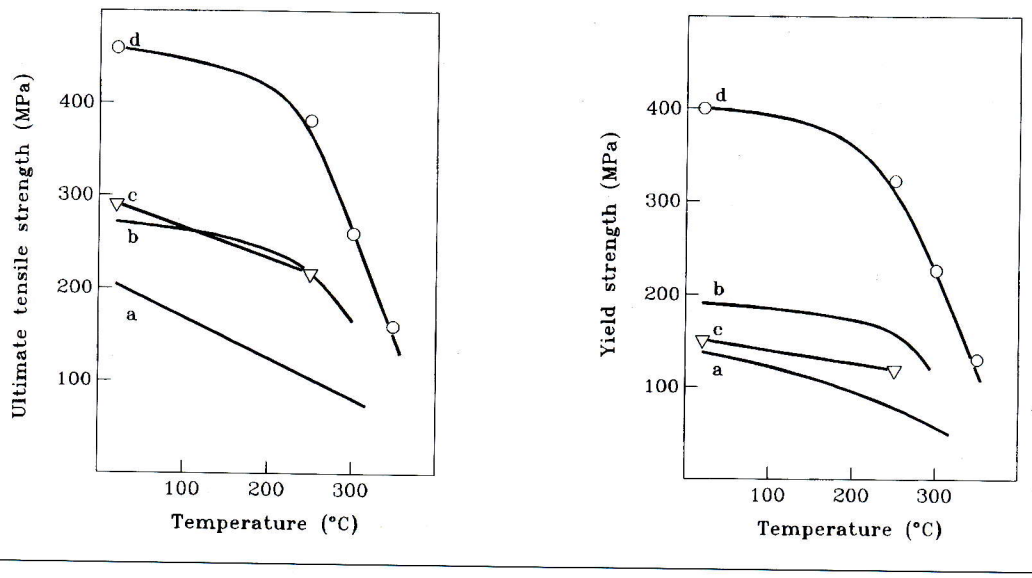

Figure 7: Tensile mechanical properties of selected magnesium-rare earth alloys versus temperature. (From ref. [4]). a: AE42; b: WE43; c: Mg-Sm6 (T6) alloy; d: Mg-Gd9.3Y4.8Mn0.6 (T6) alloy. (The AE42 and WE43 values are shown for comparison)

Magnesium-yttrium-lanthanide alloys

These alloys have high tensile strengths and yield strengths and they exhibit good properties at temperatures up to 300°C and 250°C, respectively. The WE54 alloy retains its properties at high temperature for up to 1000 h, whereas WE43 retains its properties at high temperature in excess of 5000 h. Both WE54 and WE43 have good castability and weldability, but they require solution and ageing heat treatments to optimise their mechanical properties. They are relatively expensive because of their yttrium content. Both alloys are corrosion-resistant, with corrosion rates similar to those of the common aluminum-base casting alloys.

Magnesium-rare earth- zirconium alloys

These alloys are used at temperatures between 175 and 260°C. Their high-temperature strength exceeds that of the magnesium-aluminium-zinc alloys (thinner walls can be used). The magnesium-rare earth-zinc-zirconium alloy EZ33A has good strength stability when exposed to elevated temperatures. This alloy is more difficult to cast in some designs than magnesium-aluminium-zinc alloys; its castings, however, have very good pressure tightness. Alloy ZE41A is similar to EZ33A, but it has higher tensile and yield strength because of its higher zinc content. To higher mechanical properties of ZE41A a reduction corresponds, however, in castability and weldability

The alloy EZ33A-T5 can be successfully substituted for AZ92A-T6 at high temperature. The results of creep tests of separately cast bars of the two alloys can be summarised in the following data (stress values for 0.1% creep in 1000 h):

Alloy	AZ92A-T6	T = 205°C	MPa 6.9
	"	T = 260°C,	MPa 2.1
Alloy	EZ33A-T5	T = 205°C,	MPa 58
		T = 260°C,	MPa 26
	"	T = 315°C,	MPa 8.3

An important contribution to the knowledge of Mg-rare earth-zirconium alloys has recently been given by a group of Japanese scientists. Ageing characteristics and high temperature tensile properties of magnesium alloys containing heavy rare earth elements have been studied by Kamado et al. [5]. From the results of observations using transmission electron microscopy it is found that precipitation sequences of Mg-Gd(Dy)-Nd-Zr and Mg-Gd-Y-Zr alloys are β" (Mg_3Cd-type; $D0_{19}$ type) → β' (side-centred orthorhombic) → β (face centred cubic) or β" → β'→ body centred cubic, respectively. In different papers ageing characteristics and tensile properties of Mg-Gd-Y-Zr alloys have been discussed [6, 7] and also deformation characteristics and tensile properties of forged Mg-R-Zr [8] and Mg-Gd-Y-Zr [7] alloys. Corrosion behaviour of Mg-alloys containing heavy rare earth elements has been described by Nakatsugawa et al. [9]. The corrosion rate (in 5 mass% NaCl solution saturated with $Mg(OH)_2$) of the alloy seems to be greatly reduced by the presence of rare earths: especially the addition of Nd is effective.

Magnesium-rare earth-silver casting alloys

The presence of silver improves the room-temperature strength of magnesium alloys. When rare earth elements or thorium is present, along with silver, elevated-temperature strength is also increased. The QE22A and EQ21A alloys show high tensile strength and yield strength with fairly good properties at temperatures up to 205°C. Alloy QH21A has similar properties to QE22A and EQ21 at room temperature and superior properties at temperatures from 205°C up to 260°C. The alloys QE22A, EQ21A and QH21A have good castability and weldability. To achieve higher mechanical properties, however, solution and ageing heat treatments are needed.

Magnesium-rare earth-zinc alloys

Alloys that contain high zinc levels such as ZK51A, ZK61A, ZK63A and ZH62A develop the highest yield strengths of the casting alloys and can be cast into complicated shapes. Because ZK61A has a higher zinc content, it has significantly greater strength than ZK51A. Both alloys maintain high ductility after the ageing treatment T5. The strength of ZK61A can be further increased (3 to 4%) by solution treatments plus T6 ageing treatment, without impairing ductility. These alloys have fatigue strength similar to that of the magnesium-aluminium-zinc alloys, they are, however, more susceptible to microporosity and hot cracking, and are less weldable. Addition of either thorium or rare earth metals overcomes these deficiencies. Similar properties are shown by ZE63A.

The ZE41A alloy was developed to meet the growing need for an alloy with medium strength, good weldability, and improved castability in comparison with AZ91C and AZ92A. It has good fatigue and creep properties and maximum freedom from microshrinkage.

Mg-R BINARY SYSTEMS

Intermediate Phases and Crystal Structures Stable Phases

The up-to-date information available on the crystallochemistry of Mg alloys (intermediate phases formed and structural types existing in these systems at various stoichiometries) with the rare earth metals has been summarised in Fig. 8, in which, for a better comparison, trivalent and divalent rare earth metals have been separately indicated, and data relevant to the alkaline -earth metals have been also included. Analogies between Eu and Sr, Ba and between Ca and Yb are then evident.

The structural type is defined by means of a well-known substance ("the prototype") having the given type of structure and the so-called Pearson symbol, formed by a sequence of a small letter, defining the crystal system (c= cubic, h= hexagonal, t= tetragonal, o= orthorhombic, etc.), a capital letter defining the lattice type (P= primitive, I= body centred, F= face centred, R= rhombohedral, etc.) and a number corresponding to the atoms contained in the unit cell. (A symbol such as cP2-CsCl, for instance, means that in the CsCl type structure there are 2 atoms in a cubic primitive unit cell). For more details about crystal structures of intermetallic phases, their representation and some characteristics, see also ref. [10].

Following comments to Fig. 8 may be noteworthy: the RMg compounds form in all the systems and have the CsCl type structure. The RMg_2 compounds are also formed in all these systems and have a Laves type structure. They change their structure, however, from the cubic ($MgCu_2$-type) to the hexagonal ($MgZn_2$-type) Laves type with the increase in the atomic number of the rare earths; this is in agreement with other series of RMe_2 phases (Me=metal) showing these two Laves type structures. Yttrium, according to its atomic dimensions behaves as the heavy lanthanides. The high stoichiometric ratios, such as 12:1, 17:2, 41:5, 24:5, observed in several of the reported systems, are characteristic of the alloying behaviour of metals such as lanthanides, actinides, alkaline earths.

A progressive decrease in the number of compounds and in the stoichiometries of the phases richest in Mg is evident,

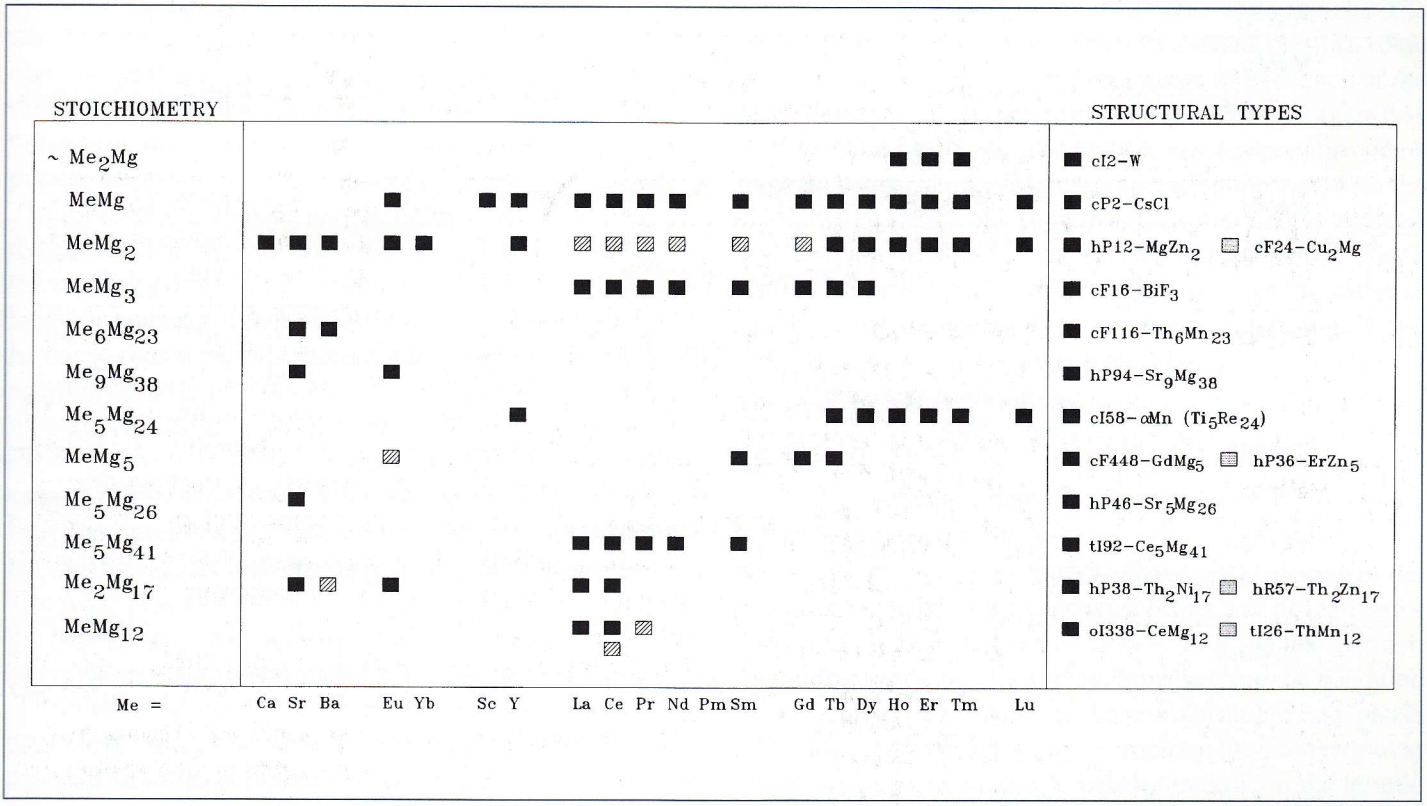

Figure 8: Stoichiometries and crystal structures of binary Mg phases formed with the alkaline earth metals (Ca, Sr, Ba), the divalent rare earth metals (Eu and Yb), here separately shown, and the trivalent R (Sc, Y and the lanthanides)

on passing from the light to the heavy rare earths (from La to Lu), this may be related to the correlation between the decrease in the atomic radius ratio r_R/r_{Mg} and the decrease in the coordination number of Mg around R. Table 4 shows, for selected structural types, the coordination typically found in binary $MeMg_x$ phases of Mg with alkaline earths and rare earth metals, by using special codes. As here below explained, we notice that high coordination numbers are usually observed: generally 12 around Mg and from 14-16 to 18-20, according to increasing values of the stoichiometric ratio, x, around Me.

The different atomic environment types observed and summarised in Table 4 are identified by their coordination polyhedra. The coordination polyhedron of an atom is the polyhedron, the vertices of which are defined by the atoms surrounding this atom. The different polyhedra are indicated by means of a "polyhedron code" which identifies the geometrical characteristics of each vertex and based on the number (and type) of the faces (triangles, squares, pentagons, hexagons, etc.) that join each other in the different vertices (coordinating atoms). The polyhedron code gives the number of equivalent vertices with the number of faces in the above-mentioned sequence as an exponent. For example, a quadratic pyramid (having 4 side triangular faces and 1 square base) has 4 (base) corners adjoining 2 triangles and 1 square and 1 corner adjoining 4 triangles: its code, therefore, is $4^{2.1.0.0}1^{4.0.0.0}$ (or briefly $4^{2.1}1^{4.0}$) with coordination number 5. The cube having 8 equivalent vertices, in each of which 3 square faces meet (no triangle), has the code $8^{0.3}$.

A more complex example may be given by the code of one of the so-called Frank-Kasper polyhedra which represent typical coordinations observed, for instance, in the Laves phases. One of these codes is $(12^{5.0}4^{6.0})$ which indicates the coordination 16. (For the $MeMg_2$ Laves phases this corresponds to 16 (Me + Mg) atoms around each Me; the index 1/3 reported in Table 4 indicates the fraction of atoms which are surrounded by this polyhedron).

TABLE 4 - Structures and coordination of selected $MeMg_x$ phases (Me = alkaline earth and rare earth metal).

Selected Stoichiometry	Structure type Pearson Symbol and Prototype	Codes of the coordination polyhedra Around Me	Around Mg
MeMg	cP2-CsCl	$(8^{0.3}6^{0.4})_{1/2}$	$(8^{0.3}6^{0.4})_{1/2}$
$MeMg_2$	Laves phases hP12-$MgZn_2$ or cF24-$MgCu_2$ or hP24-$MgNi_2$	$(12^{5.0}4^{6.0})_{1/3}$	$(12^{5.0})_{2/3}$
$MeMg_3$	cF16-BiF_3	$(8^{0.3}6^{0.4})_{1/4}$	$(8^{0.3}6^{0.4})_{3/4}$
Me_6Mg_{23}	cF116-Th_6Mn_{23}	$(8^{4.1}4^{5.0}4^{2.2}1^{0.4})_{24/116}$	$(12^{5.0})_{56/116}(6^{5.0}3^{4.1}3^{2.2}1^{0.3})_{32/116}$ $(8^{0.3})_{4/116}$
Me_9Mg_{38}	hP94-Sr_9Mg_{38}	$(8^{4.1}6^{5.0}2^{2.2}1^{6.0})_{12/94}$ $(6^{6.0}4^{5.0}4^{3.1}2^{4.2}2^{4.0})_{6/94}$	$(12^{5.0})_{44/94}(6^{5.0}3^{6.0}3^{4.0})_{12/94}$ $(7^{5.0}4^{4.1}1^{2.2}1^{1.2})_{12/94}$ $(3^{5.0}3^{3.0}1^{6.0})_{4/94}(9^{5.0}3^{6.0}1^{3.0})_{4/94}$
Me_5Mg_{24}	cI58-Ti_5Re_{24}	$(12^{5.0}4^{6.0})_{10/58}$	$(12^{5.0})_{24/58}(8^{5.0}2^{4.1}2^{3.1}1^{6.0})_{24/58}$
$MeMg_5$	hP36-$ErZn_5$	$(6^{2.2}4^{5.0}4^{4.1}2^{6.0}2^{0.4})_{6/36}$	$(12^{5.0})_{16/36}(6^{5.0}3^{6.0}3^{4.0})^{12/36}(6^{4.0})_{2/36}$
Me_5Mg_{41}	tI92-Ce_5Mg_{41}	$(10^{5.0}7^{6.0}1^{4.0})_{8/92}$ $(8^{5.0}8^{4.1}4^{6.0})_{2/92}$	$(12^{5.0})_{32/92}(8^{5.0}2^{4.1}2^{3.1}1^{6.0})_{16/92}$ $(6^{5.0}6^{4.1}2^{3.1}1^{6.0})_{16/92}(6^{5.0}3^{4.0}1^{6.0})_{8/92}$ $(12^{5.0}2^{6.0})_{8/92}(8^{0.3})_{2/92}$
Me_2Mg_{17}	hP38-Th_2Ni_{17}	$(12^{4.0.0.1}6^{4.0})_{2/38}$ $(12^{4.1}6^{5.0}2^{6.0})_{2/38}$	$(12^{5.0}2^{6.0}1^{4.0})_{12/38}(8^{5.0}2^{4.1}2^{3.1})_{12/38}$ $(12^{5.0})_{6/38}(12^{5.0}2^{6.0})_{4/38}$
	hR57-Th_2Zn_{17}	$(9^{4.1}3^{3.1}3^{5.0}3^{4.0}1^{6.0})_{6/57}$	$(12^{5.0}2^{6.0}1^{4.0})_{18/57}(8^{5.0}2^{4.1}2^{3.1})_{18/57}$ $(12^{5.0})_{9/57}(12^{5.0}2^{6.0})_{6/57}$
$MeMg_{12}$	tI26-$ThMn_{12}$	$(8^{5.0}8^{4.1}4^{6.0})_{2/26}$	$(12^{5.0})_{8/26}(12^{5.0}2^{6.0})_{8/26}$ $(8^{5.0}2^{4.1}2^{3.1})_{8/26}$

Metastable Phases

Metastable phases and structures have been described for several Mg-R systems. Those formed in the Mg-rich alloys may be particularly interesting. In the Mg-Ce system [11] various crystal structures have been suggested for the composition range $Ce_{10-12}Mg_{90-88}$ (order-disorder relationships may be involved and possibly metastable phases. Further study is needed). In the Mg-Dy system (as an example of the alloys with the heavy R) the appearance of an ordered phase inside the Mg solid solution has been observed in the first stage of age hardening. It has the hexagonal hP8-Mg_3Cd type structure (also called, using the old, and somewhat obsolete, Struktur-Bericht notation, a $D0_{19}$ type structure) [12]. With continued ageing (in a second stage) hardening increased substantially to a maximum, with the precipitation from the ordered regions, of an orthorhombic metastable phase (as plates parallel to the basal plane, of the matrix, probably coherent with it). In the third stage, finally, the alloy overaged with the precipitation of the stable Dy_5Mg_{24} phase. In the Mg-Y system, at various stages of ageing of the supersatured Mg solid solution, ordering of the hP8-Mg_3Cd type was observed. With prolonged holding at the ageing temperature of 250 °C an orthorhombic structure was observed [13].

Phase Diagrams of the Rare Earth-Magnesium Binary Systems

The stability of the different R-Mg phases (and indeed, their melting behaviour and formation mechanism) may be highlighted considering the stable phase diagrams of the various R-Mg systems. They are reported in Figs. 9 and 10. A number of these have been studied in our laboratory: Mg-Pr [14], Mg-Nd [15], Mg-Sm [16], Mg-Tb [17], Mg-Dy [18], Mg-Ho [19], Mg-Er [20], Mg-Tm [21], Mg-Sc [22]. They were studied by using differential thermal analysis, X-ray powder diffraction, optical and scanning electron microscopy, electron probe microanalysis. Details on the laboratory preparation techniques (induction melting inside special tantalum crucibles sealed by arc welding, etc.), have been reported, for instance, in refs. [14,18].

The following comments may be noteworthy: as for the systems formed by Mg with the trivalent rare earths (see Fig.9), the melting points of the intermetallic phases are not very high in comparison with those of the component elements. In the R-rich regions a large solid (body-centered cubic) solution field is present, which is connected to the high temperature modification of the rare earth metal itself, when it exists. For some heavy rare earths (Ho, Er, Tm, Lu) no allotropic modifications are known and in these cases the bcc fields are intermediate binary fields, corresponding to a binary composition range typically centred around 33 at% Mg. The RMg phases form peritectically for La and Ce and for the heavy rare earth metals starting from Gd, while for the intermediate metals the melting is congruent. The RMg_2 phases show peritectic formation for all the rare earths with the exception of Sm for which a congruent melting is proposed. The RMg_3 compounds form congruently from La to Nd, peritectically for Gd and Tb and through a solid state reaction, peritectoidal equilibrium, for Dy. The Mg-richest compounds, at high stoichiometric ratio, all form peritectically. The progressive variation from La-Mg to Lu-Mg of the relative thermal stability of the RMg and RMg_3 phases is apparent.

The Sc-Mg system is very different from the previous ones; this is probably related to the smaller atomic dimensions of scandium with respect to the other rare earth metals. The Sc-Mg phase diagram, not completely studied, presents some uncertainties (equilibria involved, range of existence of the phases) especially in the region around 50 at% (possibly corresponding to the formation of a low temperature intermediate phase). The Y-Mg diagram (in connection with the similarity in the atomic dimension) shows a close analogy with those of the heavy rare earths: compare also with Fig.9. On the other hand the different behaviour of the divalent rare earths (Eu and Yb) is clearly noticed from Figs 8 and 10. The close analogy between the Yb-Mg and Ca-Mg systems is apparent from Fig. 10.

A summary of all the main phase diagram features of the Me-Mg systems is given in Fig. 11, in which the projections of the phase diagrams onto the composition axis are reported and compared.

It is well known that generally we have, as a function of the R atomic number, a smooth trend of several properties of the alloys formed by the different R with a given partner. The properties to be considered, however, are the so-called constitutional characteristics (phase formulae and phase structures, phase diagrams and formation thermodynamics) which may be considered dependent mainly on the atomic dimensions. More complex, of course, is the trend of prop-

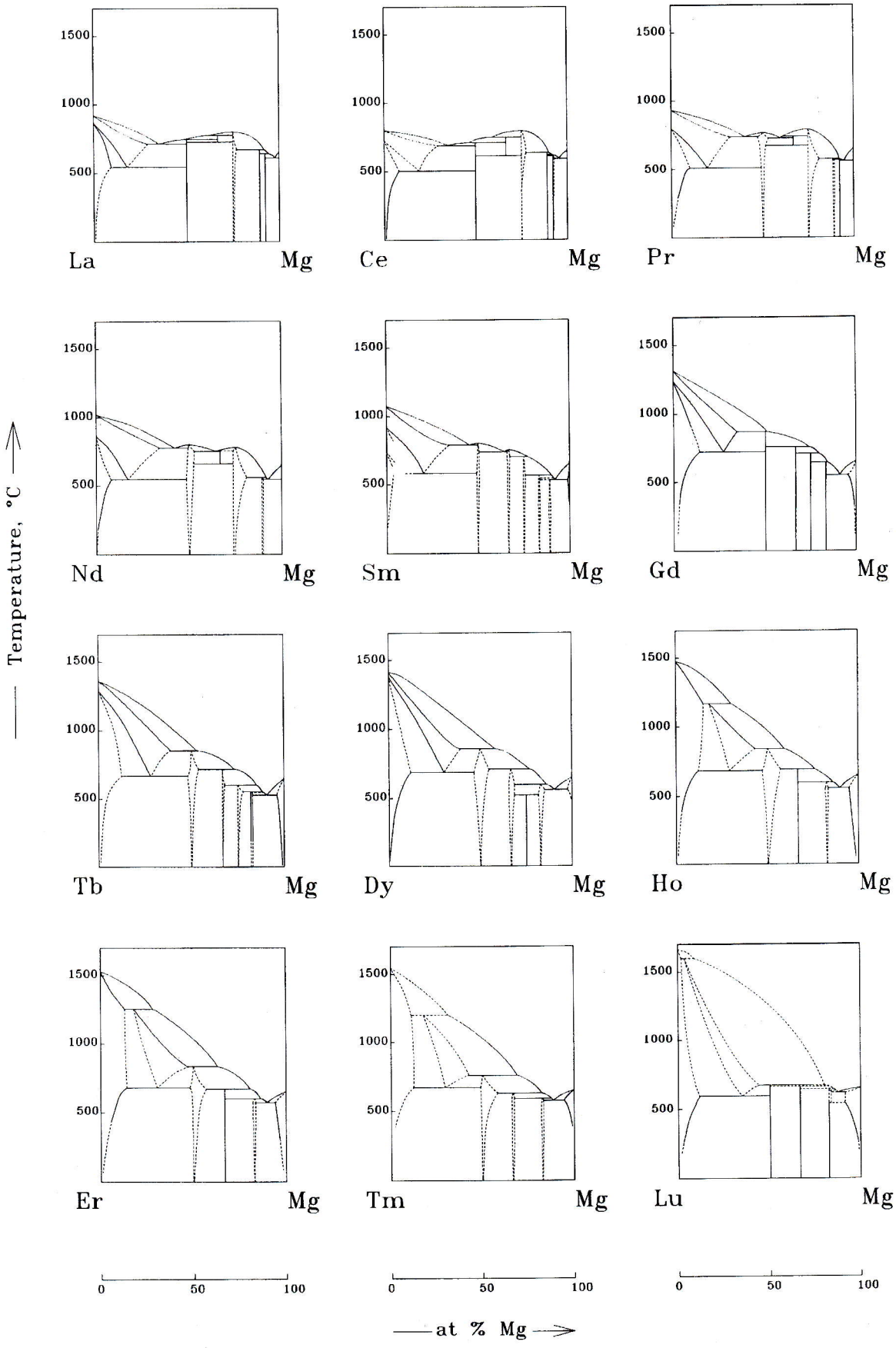

Figure 9: Phase diagrams of R-Mg systems of the trivalent lanthanides

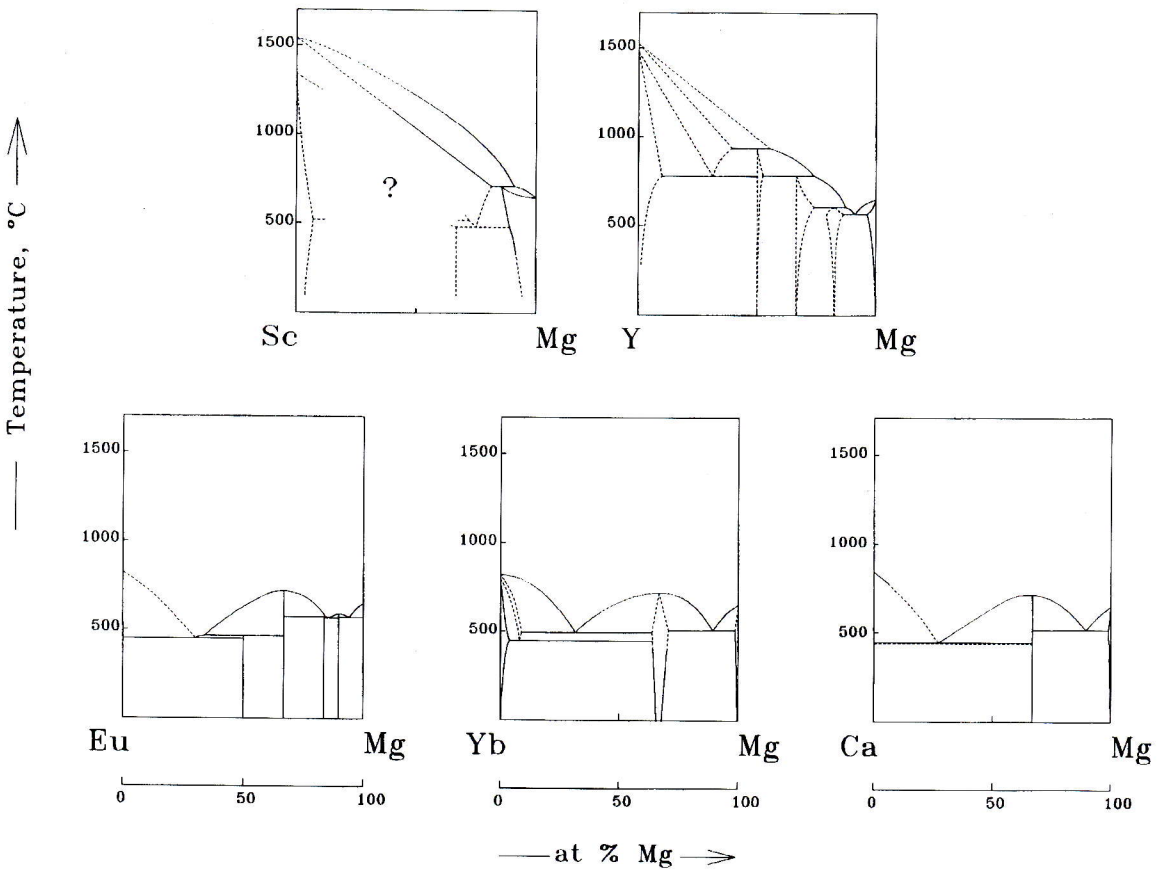

Figure 10: Binary phase diagrams of Mg with Sc and Y, with the divalent rare earth metals (Eu, Yb) and with Ca (representative of alkaline earth metals), added here for a better comparison with Yb

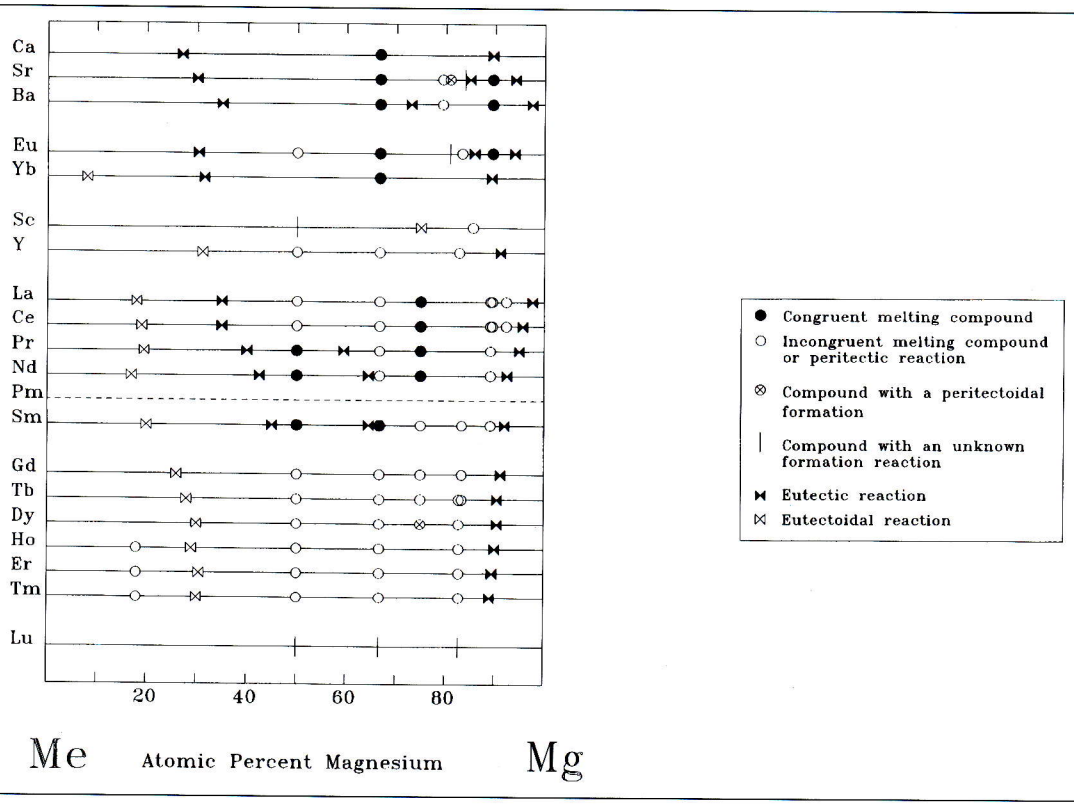

Figure 11: Schematic, comprehensive, representation of the melting behaviour of the binary alloys of magnesium with the alkaline earth metals and of magnesium with the rare earth metals. The projections of the equilibrium (liquidus) lines onto the composition axis are shown

erties such as electronic, magnetic, etc., which are related to the actual electronic configuration. An example of the even progression along the rare earth series of a "constitutional" property of R-Mg alloys is presented in Fig. 12, in which the so-called reduced melting temperature is given. According to Gschneidner [23], it is defined as the ratio of the melting points of the compound and of the rare earth metal involved (both in Kelvin degrees). We notice, for all the compounds reported, a similar pattern which is typical of nearly all the compound series formed by several metals with the rare earths. Notice, however, that the divalent rare earth, Eu and Yb, often show strong deviation from such trend. Other parameters (beside the mentioned reduced melting temperature) have been used or devised to highlight the regular trends of various properties and the links between them. Special attention has been, for instance, dedicated to the analysis of the trends of the temperatures (and compositions) of invariant equilibria or of heats of formation, lattice parameters, volume contractions, etc.).

These trends may be useful for an over-all checking of the data and/or for the prediction (by interpolation) of unknown values. This point has previously been discussed, for instance, in refs. [24-27] and in the specific case of the Mg alloys in refs. [21] and [28].

Fig. 13 shows the relationship for one of the R-Mg systems, Gd-Mg, between different constitutional properties. Moreo-

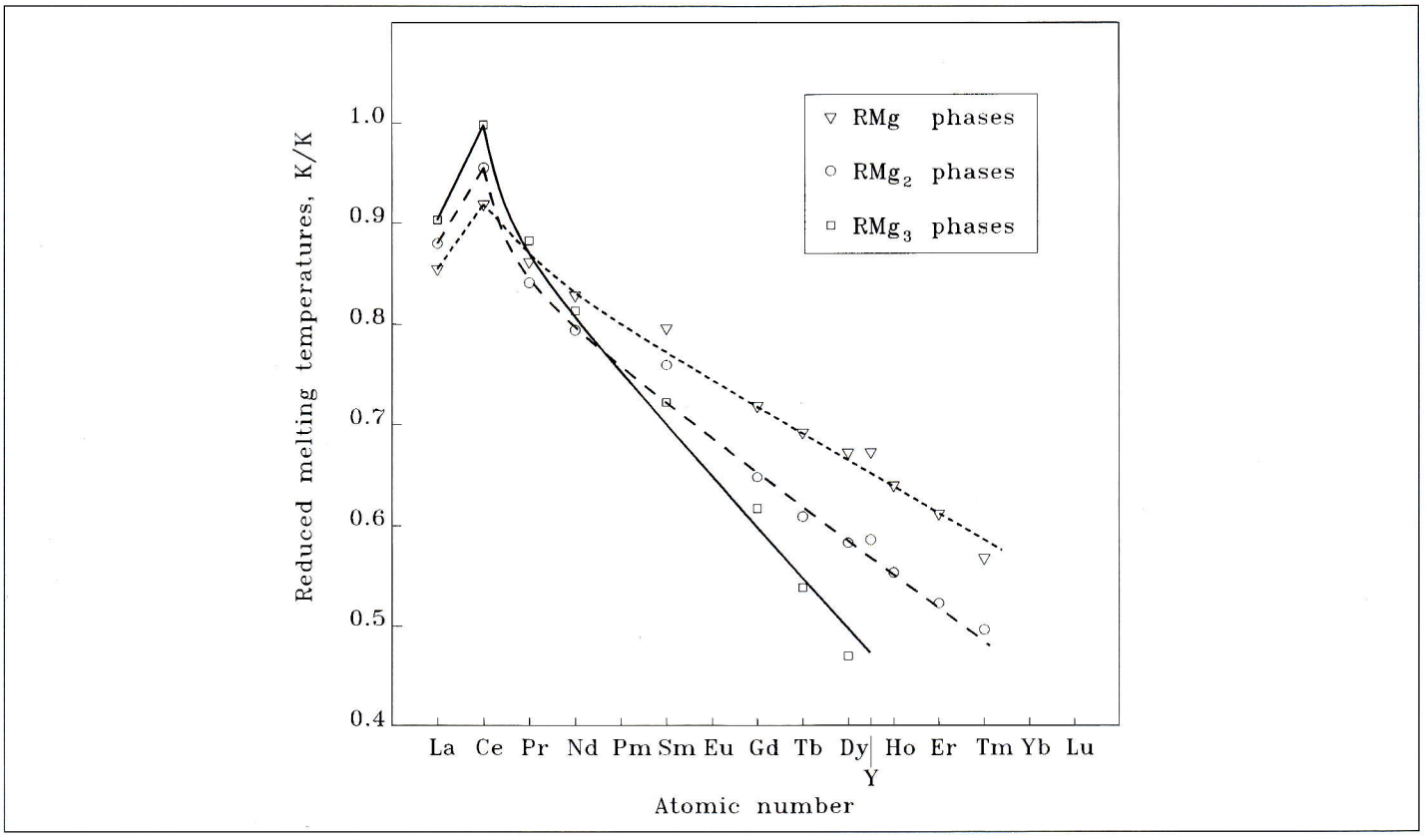

Figure 12: Trends of the reduced melting temperatures versus the atomic number of the trivalent rare earth for the compound series RMg, RMg_2 and RMg_3. The reduced temperature is defined as the ratio of the melting temperatures (in kelvin) of a certain compound and of the corresponding involved rare earth metal

ver, the similar trends versus composition of the ΔH of formation of a few R-Mg alloys are shown and compared with the values calculated for the Gd-Mg system [29]. In the same figure, the experimental phase diagram of this system is compared with the "computed" version, obtained by using the Calphad method [33-34]. Phase diagram and thermodynamics are indeed strongly correlated and appropriate calculation techniques have been implemented (Lukas program [35-36], Thermocalc [37]) to optimise and assess the experimental data. The so-called Calphad (Calculation of Phase Diagram) techniques have been greatly perfected and are widely used in the optimisation, check, calculation and prediction of phase equilibria in even complex systems (both of metal alloys and ceramic materials). In international scientific circles, a great interest has developed in these techniques and their basic theories and applications, which can be seen from the many papers, congresses, etc., on the subject.

As for simple systems such as the binary ones, a sound assessment of their diagrams is very important also because the optimised data may be used as a reference for extrapolation to more complex systems, containing addition of other metals to the two components, and prediction of the equilibria involved. To this end, the knowledge of the thermodynamics of the alloys is necessary: in the case of the R-Mg alloys these data are scant and, often, seem to be unreliable. Work is needed along these lines.

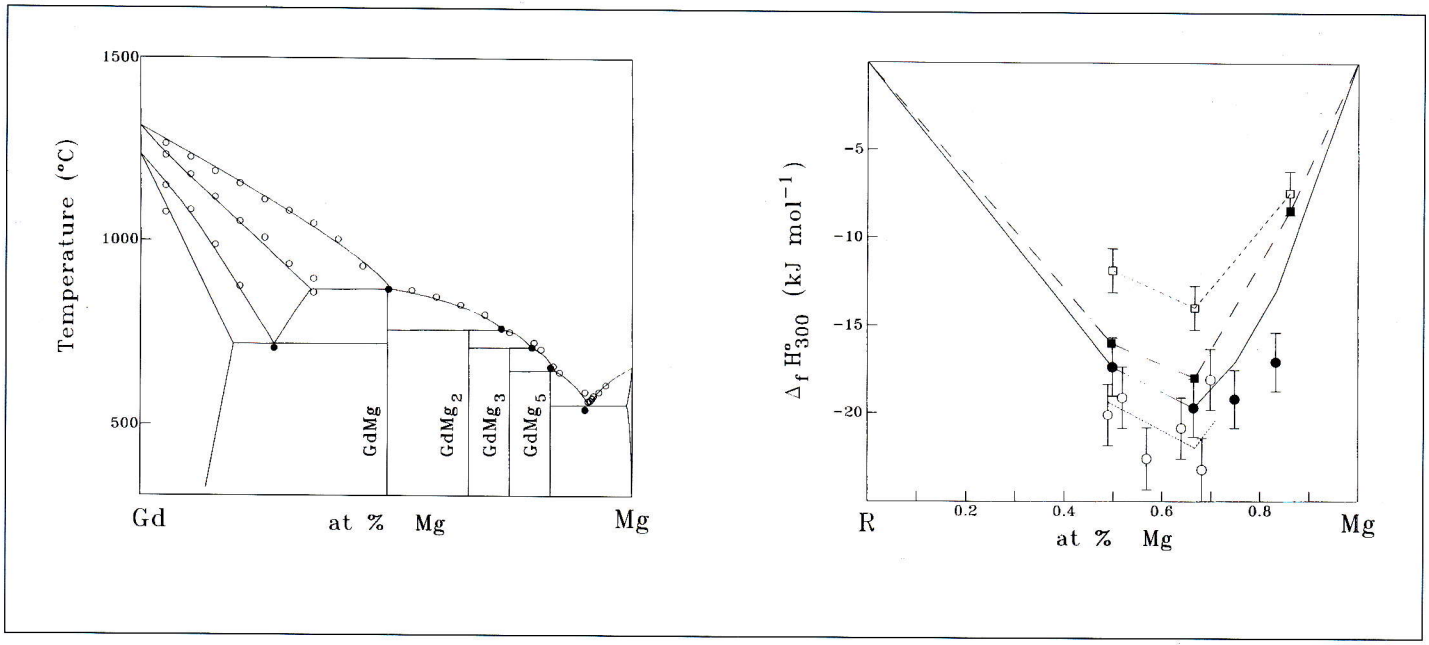

Figure 13: Gd-Mg system. a) Comparison between the computed phase diagram (continuous line) and the experimental points (•, invariant equilibria;○, two phase equilibria) [29]. b) Calculated standard enthalpy of formation ($\Delta_f H°$), at 300 K, of the Gd-Mg solid alloys (continuous line) compared with computed values (■) of the Y-Mg system [30] and with the experimental $\Delta_f H°$ of a few R-Mg alloys: ○, Sm-Mg system, calorimetric data [16], •, Gd-Mg system, from vapour pressure measurements [31];□, Y-Mg system, from acid solution [32]

Mg-RICH REGIONS AND Mg-SOLID SOLUTIONS

The Mg-rich regions of binary and ternary systems of magnesium containing rare earths metals are especially interesting in view of the possible technical applications of R-containing Mg alloys.

A number of papers deal with the extensions of the Mg-solid solutions; these have been determined for the different Mg-R systems by using several experimental methods such as X-ray parametric data, micrographic appearance, resistometric measurements, etc., even though the reported data are often conflicting.

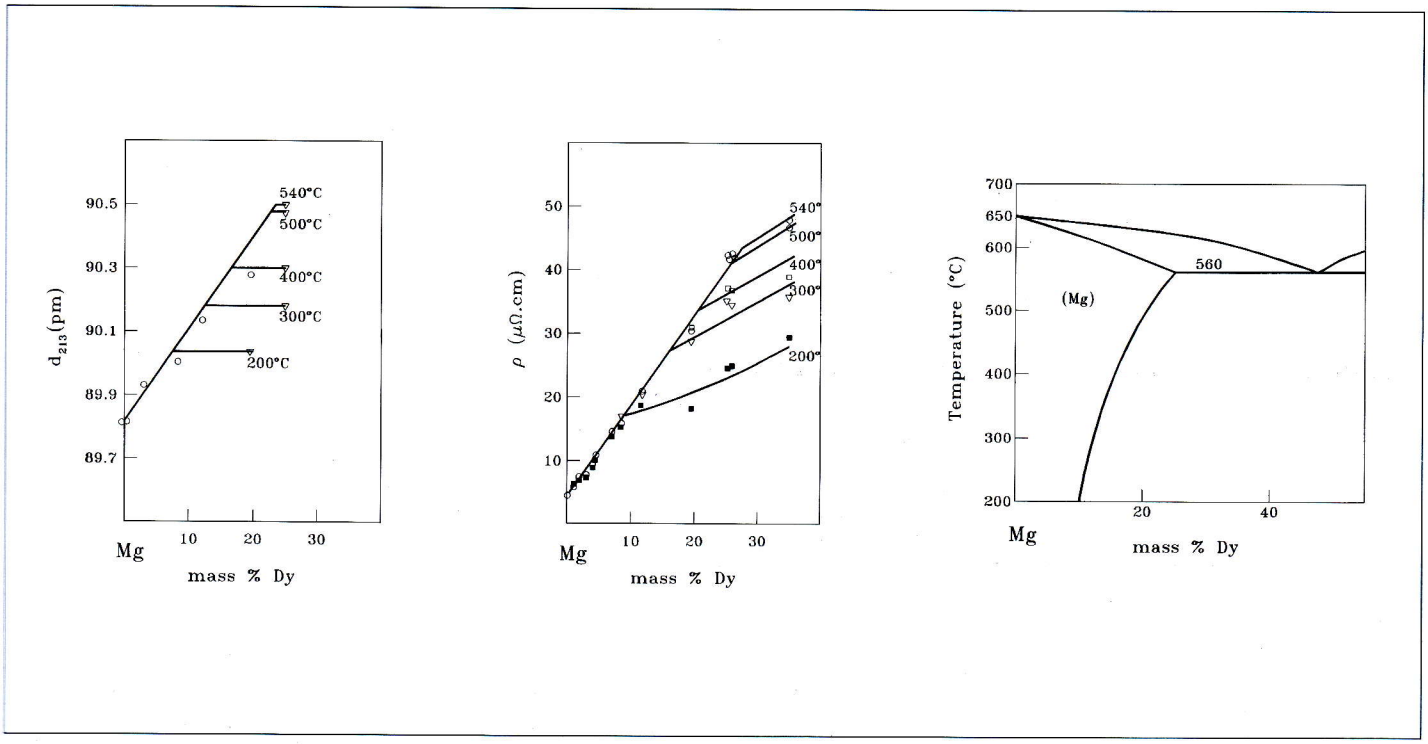

Figure 14: Mg-rich region of the Mg-Dy system. (Notice that in comparison with the other figures, the composition is here given in mass %). The solubility limit of Dy in the Mg solid solution is compared with the trends, at different temperatures, of the lattice parameters (here averaged by the trend of the interplanar spacing d corresponding to the (213) planes) and of the electrical resistivity. (From ref. [38])

The observed changes of the unit cell dimension by additions of rare earth metals have been studied. In many cases only data concerning the averaged variation of the unit cell dimensions have been reported as exemplified in Fig. 14 relative to the Mg solid solution of the Mg-Dy system [38]. In this figure we may see the trend observed for the spacing d of the lattice planes corresponding to a certain Miller index (2 1 3 in the example). In the case of the Mg-Sc system however, data concerning the change of the unit cell edges, a and c, of Mg, by addition of Sc, have been reported in the literature [39]. (See Table 5).

Fig.15 show the trend of the solid solubility of different rare earths in Mg (in atom %), as suggested by Rokhlin [38]. Notice the gradual increase of solubility on passing from the light to the heavy rare earths. This may be related to the progressive decrease of the rare earth metallic radius (see Fig. 2) which becomes nearer to that of Mg (160.2 pm). Fig. 15 may be compared with Fig.16 which shows the trend of the resistivity versus the R percentage [40].

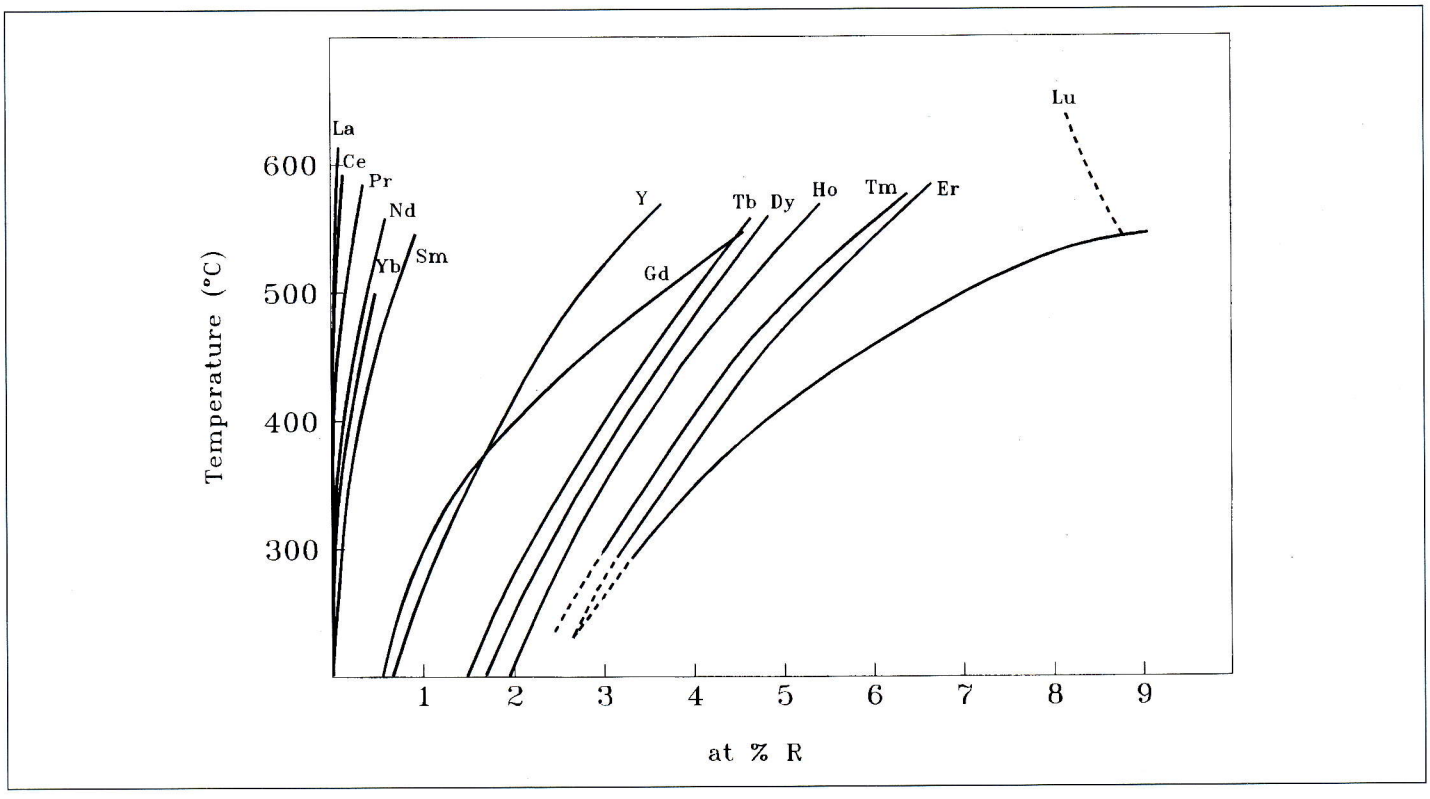

Figure 15: Trends of solid solubility limits versus temperature of several rare earth in magnesium

TABLE 5 - Mg-Sc system: lattice parameters of the (Mg) solid solution at 25°C (from [39])

Composition at % Sc	Lattice parameters (pm) a	c	c/a
0	320.90	520.93	1.6233
3	321.18	520.80	1.6215
6	321.44	520.33	1.6187
	321.49	520.46	1.6189
10	321.68	520.42	1.6178
	321.65	520.34	1.6177
15	321.82	520.35	1.6169

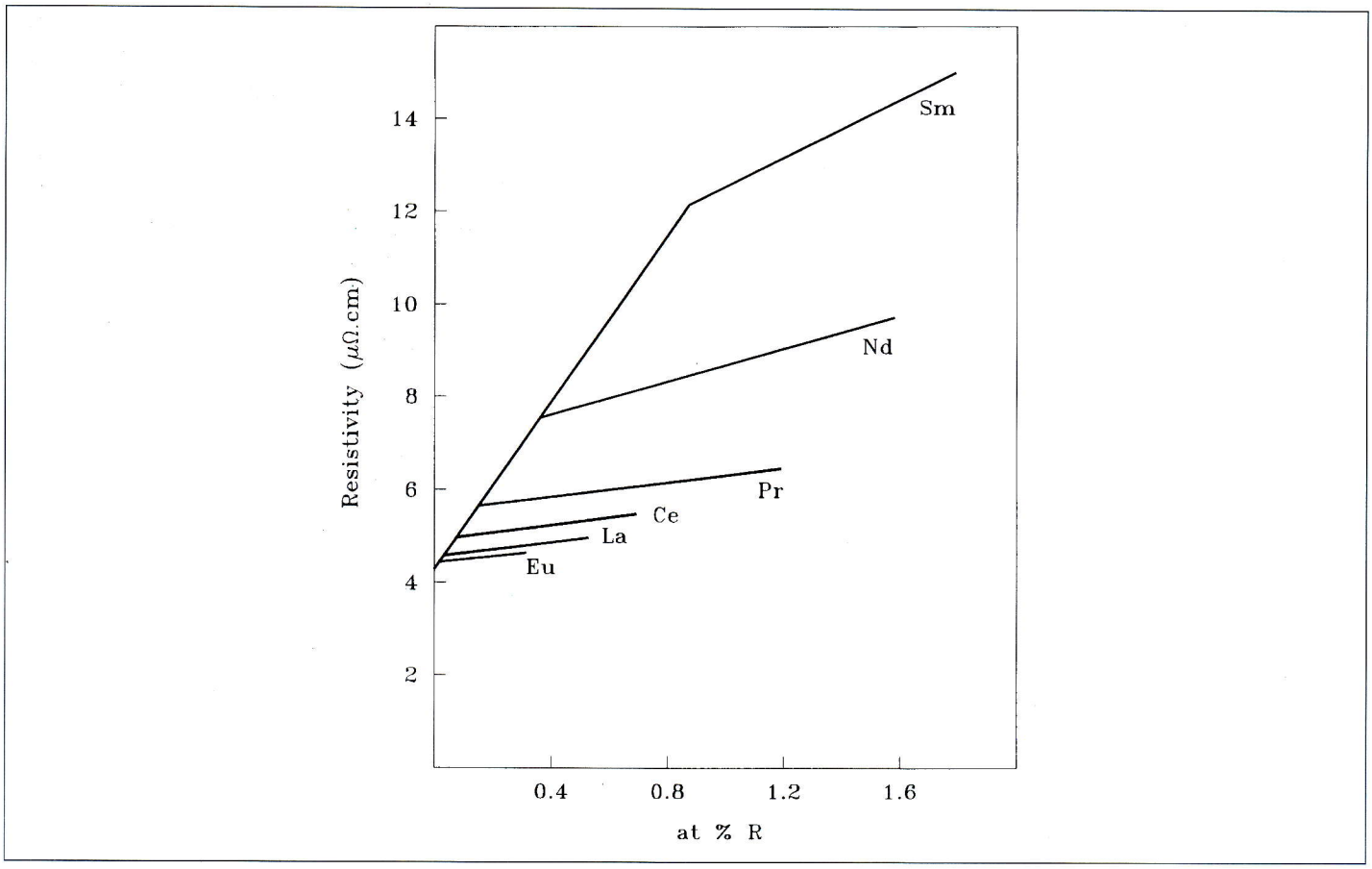

Figure 16: Solid solutions of the rare earth metals in magnesium . Trends of electrical resistivity (at 500°C) versus composition. Notice that the different curves practically coincide in the Mg solid solution range but extend differently in the two-phase regions beyond the specific solubility limits

TERNARY Mg SYSTEMS INVOLVING RARE EARTH METALS

Data on the constitutional properties of ternary alloys containing Mg and, at least, one of the rare earth metals, are reported in literature. At present our research group is involved in the study of systems such as Al-Mg-Sc [41] and Al-Mg-Y [42], for which preliminary results have been published.

Within the ternary Mg systems, moreover, the R'-R"-Mg alloys containing two different rare earths form a particular group for which it is possible to highlight some regularities and to extend the application of certain rules valid for binary R-alloys. In the case of binary (trivalent) R'-R" alloys, on the basis of the trends of some properties previously discussed, it has been shown that the behaviour of a certain mixture of two rare earth metals, R' and R", simulates the behaviour of another rare earth (R) having an intermediate value of the atomic number and whose atomic dimensions lie between those of R' and R". This mixture may be expected to display physical properties (constitutional properties) similar to those of the particular true lanthanide which is being simulated. For instance, by alloying La with increasing amounts of lutetium, the samples of these inter-rare-earth binary alloys, will show properties, crystal structures, etc., in agreement with those of the intermediate rare earth metal, Ce, Pr, etc. In this context, on the basis of its atomic dimensions, yttrium may be considered as nearly equivalent to Dy and Ho. Several light lanthanides may therefore be simulated also by La and Y mixtures containing increasing quantities of yttrium. This is the concept of pseudolanthanide, already defined by Gschneidner [43]. (Notice, however, that this concept applies to the constitutional properties of trivalent R). This concept has been applied to the study of ternary R'-R"-Mg alloys; in particular it has been used in order to compare series of R'-R"-Mg alloys (containing a mixture of the trivalent R' and R" in a given composition ratio) with the R-Mg binary alloys formed with a certain intermediate R. To this end the experimental data of the R-Mg binary systems have been summarised in a scheme such as that reported in Fig.17, in which, in a particular arrangement, the isothermal sections of the binary R-Mg phase diagrams are reported. The different sections are represented with the Mg vertex in common and are plotted in order of the decreasing rare earth ionic radius. The resulting diagram represents a simulation of a general R'-R"-Mg system, useful in predicting the structure of complex Mg alloys containing different rare earths. A number of R'-R"-Mg iso-

thermal sections have been experimentally studied in our laboratory: Mg-Y-La [44], Mg-Y-Ce [45], Mg-Y-Pr [46], Mg-Y-Gd [47]. The Mg-rich regions (between ~ 50 to 100 at% Mg) of these experimental diagrams and the various phase equilibria existing at 500°C are reported in Fig.18. The shaded regions represent single phase fields; the two-phase regions are included within thick lines (in these regions some tie-lines, represented by thin lines, have been determined). The three-phase fields are indicated by asterisks.

The predicted isothermal sections are in good agreement with those experimentally determined. We may notice that the different sections, for instance, of the La-Y-Mg system with increasing values of the yttrium content may be considered simulated by the different binary systems included between La-Mg and Y-Mg (Ce-Mg, Pr-Mg, etc.). Notice, moreover, that a number of different ternary systems (Ce-Y-Mg, Pr-Y-Mg, etc.) (see Figs. 11 and 17) are "contained" in the more general La-Y-Mg system.

These considerations may, therefore, be useful also as additional guidelines for planning the preparation of complex alloys and, in view of special applications, for designing their characteristics and compositions.

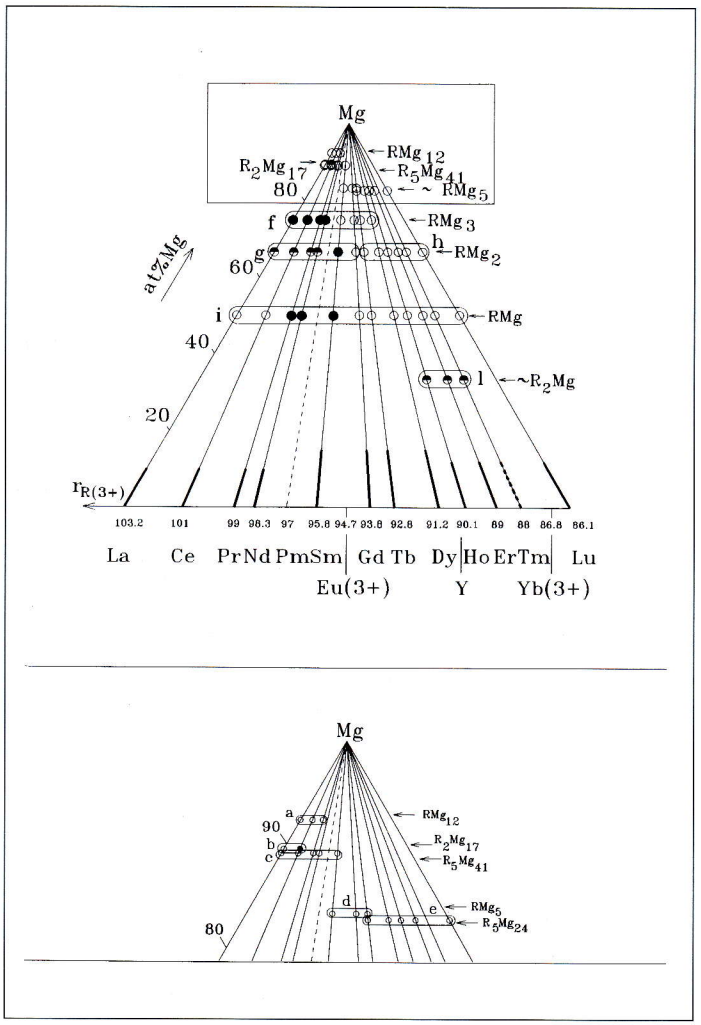

Figure 17: Isothermal, linear, sections of the R-Mg binary systems arranged in order to simulate a general R'-R"-Mg ternary systems. The Mg points of the different binary R-Mg systems are superimposed and the R points are arranged on the basis line of the triangle according to their atomic dimensions (here represented by their ionic radii). The points representing the same crystal structure have been connected in order to define a kind of "stability region" of the structure. For the same phase-type following symbols have been used: ●, congruent melting; , peritectic formation; , peritectic formation, followed by eutectoidal decomposition. (An enlarged map of the Mg-rich region is also shown)

AMORPHOUS, QUASICRYSTALLINE AND NANOCRYSTALLINE Mg-R ALLOYS

Amorphisation has achieved an important role in metallurgy because of the good mechanical, physical and chemical properties which may often be obtained. Several alloys containing R metals have been considered and the role of R additions discussed.

Recently a comprehensive monograph on amorphous, quasicrystalline and nanocrystalline alloys in Al- and Mg-based systems has been published by Inoue [48]. It contains both a description of various experimental data obtained by the authors research group and a general review of the alloys with the rare earth elements. Large space has been dedicated to the Mg-R base amorphous alloys. Several points have been especially considered which may be summarised here in order to give an idea of the properties of this group of substances.

History of the Mg-based amorphous alloys. A description is given from the very beginning up to recent results on the synthesis of these kind of alloys in ribbon, bulk, powder forms by various preparation techniques such as melt spinning, metallic mold and high pressure die castings, high-pressure gas atomisation.

Amorphous alloy systems. A summary of these systems includes Y-Mg, R-Mg-Al, R-Mg-Ni, R-Mg-Cu, R-Mg-Zn alloys.

Mechanical properties. The trends and the improvement of several properties such Young's modulus, tensile fracture strength, Vickers hardness are discussed. The good bending ductility of several Mg-based amorphous alloy is emphasised.

Glass transition and supercooled liquid. The crystallisation temperature of R-Mg-Me alloys of transition metals generally is in the range from ~ 170°C to 330°C. The R-Mg-Me amorphous alloys show a distinct glass transition followed by a large supercooled liquid region and then by crystallisation. The trends of crystallisation temperature T_x, glass transition temperature T_g and $\Delta T_x = T_x - T_g$ have been discussed.

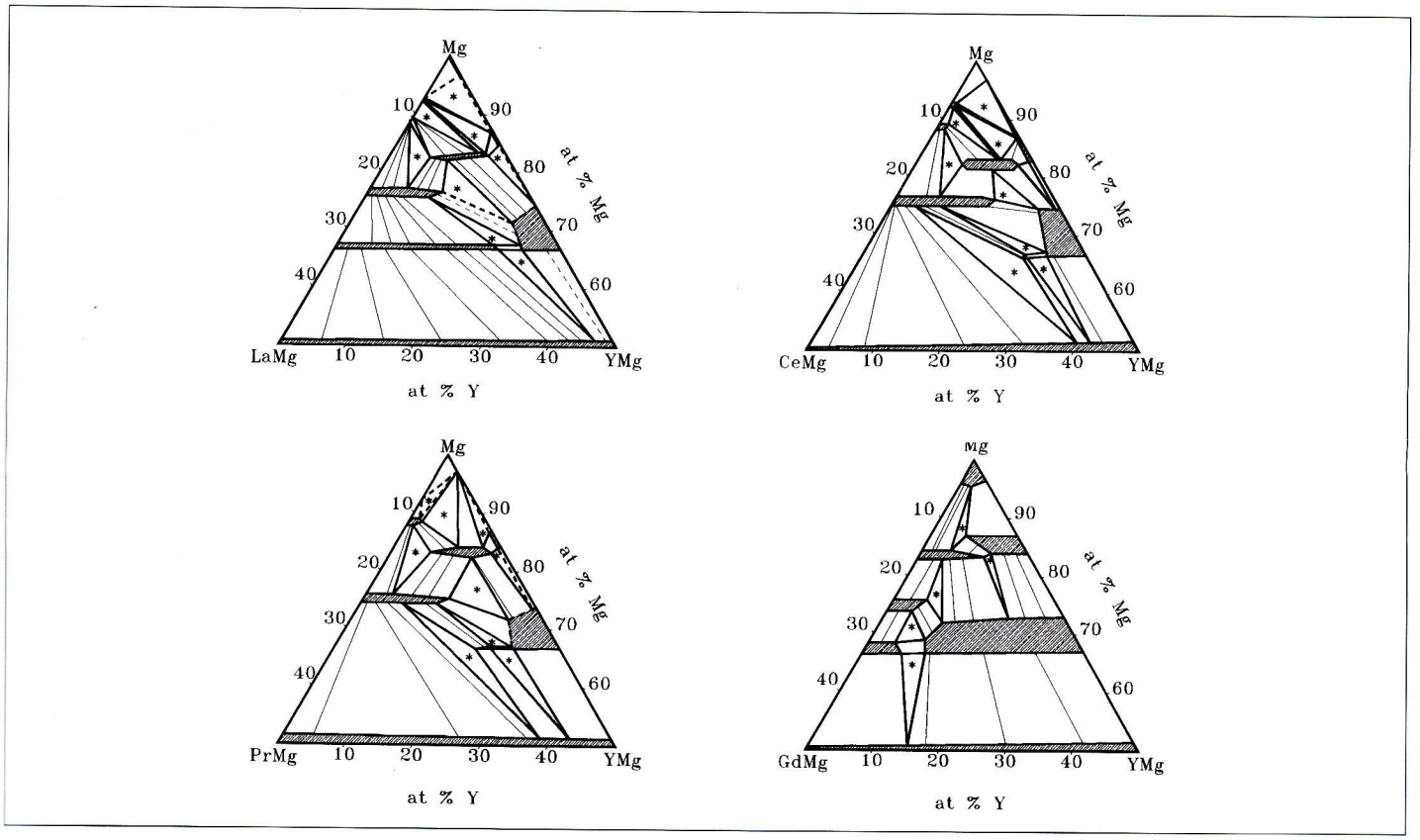

Figure 18: Experimental isothermal sections (at 500°C and from 50 to 100 at% Mg) of a few Y-R-Mg systems. Notice that the single phase fields (represented by the shaded areas) correspond to the regions defined in Fig. 17. The gradual variation of the single phase regions, on passing from the alloys with La to those with Ce, Pr, Gd, is evident

Crystallisation behaviour. The behaviour of $R_{10}Mg_{65}Cu_{25}$ alloys is described. For alloys having large ΔT_x, as with Y and Tb, the amorphous crystallises in a single stage corresponding to the simultaneous precipitation of more than two type of crystalline phases. The crystallisation takes place through two stages for Sm and Nd and three stages for Yb according to a significant decrease of ΔT_x.

Large glass-forming ability. The dependence of glass forming ability on ΔT_x is discussed. The extremely high glass-forming ability of amorphous alloys in some R-Mg-Me systems with high ΔT_x, such as in the Mg-Cu-Y system is evidenced and related to the high resistance of the supercooled liquid against crystallisation.

Structure analysis. The results of the examination of amorphous $La_{20}Mg_{50}Ni_{30}$ alloys by using the amorphous X-ray scattering are reported and discussed.

Properties, preparation equipments and schemes of production systems of bulk amorphous alloys produced by casting, of bulk amorphous alloys produced by atomisation and extrusion techniques and bulk crystalline alloys produced by atomisation and extrusion techniques are also described.

Results on Mg-based amorphous alloys containing nanoscale Mg particles and Mg-based quasicrystals containing R elements are finally summarised in this review by Inoue [48].

ACKNOWLEDGEMENT

Several topics and development of this work have been performed in the framework of the Italian Progetto Finalizzato "Materiali Speciali per Tecnologie Avanzate II (PF MSTA II)".

A summary of this paper has been presented at the Italian-Japanese Seminar, in Portonovo, Ancona (September 1997). The authors, and especially R.F., express their thanks to the organisers for their support, hospitality and kind advices. Special thanks are due to Professors T.Mohri, G.Caglioti and E.Evangelista.

REFERENCES

[1] K.A.Gschneidner, Jr., B.J.Beaudry and J.Capellen. Rare Earth Metals. In *ASM Handbook, Vol. 2, Properties and Selection: Nonferrous Alloys and Special-Purpose Materials*, ASM International, 1990, pp. 720-732.

[2] E.T.Teatum, K.A.Gschneidner, Jr. and J.T.Waber. In *"Compilation of Calculated Data Useful in Predicting Metallurgical Behaviour of the Elements in Binary Alloy Systems"*, Report LA-4003, UC-25, Metals, Ceramics and Materials, TID-4500, 1968, Los Alamos Scientific Laboratory.

[3] S.Housh, B.Mikucki and A.Stevenson. Selection and Application of Magnesium and Magnesium Alloys. In *ASM Handbook, Vol. 2, Proper-*

ties and Selection: Nonferrous Alloys and Special-Purpose Materials, ASM International, 1990, pp. 455-516.

[4] G.Neite, K.Kubota, K.Higashi and F. Hehmann. Magnesium-Based Alloys. In R.W.Cahn, P.Haasen, E.J.Kramer (Eds), *Materials Science and Technology. A Comprehensive Treatment*, Vol. 8, K.H.Matucha (Ed.), *Structure and Properties of Nonferrous Alloys*, VCH, Weinheim, 1996, pp. 113-212.

[5] S.Kamado, Y.Kojima, R.Ninomiya and K.Kubota. Ageing characteristics and high temperature tensile properties of magnesium alloys containing heavy rare earth elements, *Proc. 3rd Intern. Magnesium Conference*, Manchester, UK, 1997.

[6] S.Kamado, Y.Kojima, S.Taniike, I.Seki and S.Hama. Ageing characteristics and tensile properties of Mg-Gd-Y-Zr alloys, *Proc. 4th Inter. Conf. on Magnesium Alloys and their Applications*, Wolsburgh, Germany, 1998.

[7] I.A.Anyanwu, Y.Kitaguchi, Y.Harima, S.Kamado, Y.Kojima, S.Taniike and I.Seki. Ageing characteristics and tensile properties of forged Mg-Gd-Y-Zr alloys, *Proc. 1st Israeli Inter. Conf. on Magnesium Science and Technology*, Dead Sea, Israel, 1998.

[8] I.A.Anyanwu, Y.Kitaguchi, Y.Harima, S.Kamado, Y.Kojima, S.Taniike and I.Seki. High temperature deformation characteristics and tensile properties of forged Mg-R-Zn alloys. *Proc. Intern. Symp. on Designing, Processing and Properties of Advanced Engineering Materials*, Toyohashi, Japan, 1998.

[9] I.Nakatsugawa, S.Kamado, Y.Kojima, R.Ninomiya and K.Kubota. Corrosion behaviour of magnesium alloys containing heavy rare earth elements, Proc. *3rd Intern. Magnesium Conference*, Manchester, UK, 1997.

[10] R.Ferro and A.Saccone. Structure of intermetallic compounds and phases. In R.W.Cahn and P.Haasen (Eds.), *Physical Metallurgy*, fourth, revised and enhanced edition, North Holland, Amsterdam, 1996.

[11] A.A.Nayeb-Hashemi and J.B.Clark. Cerium-Magnesium. In A.A.Nayeb-Hashemi and J.B.Clark (Eds.) *Phase Diagrams of Binary Magnesium Alloys*, ASM International, 1988, pp.78-88.

[12] L.L.Rokhlin. An investigation of the decomposition of the supersaturated solid solution in alloys of magnesium with dysprosium, *Fiz. Met. Metalloved*, 55(4) (1983), 733-738.

[13] M.E.Drits, L.L.Rokhlin and I.E.Tarytina. Specific features of the structure of solid solutions in alloys of magnesium with yttrium, *Izv. Akad. Nauk SSSR*, Met., (3) (1983), 111-116.

[14] A.Saccone, A.M.Cardinale, S.Delfino and R.Ferro. A contribution to the rare earth intermetallic chemistry: praseodymium-magnesium alloy system, *Intermetallics*, 1 (1993)131-138.

[15] S.Delfino, A.Saccone and R.Ferro. Phase relationships in the neodymium-magnesium alloy system. *Met. Trans.* 21A (1990), 2109-2114.

[16] A.Saccone, S.Delfino, G.Borzone and R.Ferro. The samarium-magnesium system: a phase diagram, *J.Less-Common Metals*, 154 (1989), 47-60.

[17] A.Saccone, S.Delfino, D.Macciò and R.Ferro. Experimental investigation of the Tb-Mg phase diagram, *J.Phase Equilibria*, 14 (1993), 479-484.

[18] A.Saccone, S.Delfino, D.Macciò and R.Ferro. A contribution to the magnesium intermetallic chemistry: dysprosium-magnesium system, *Z.Metallkde.*, 82 (1991), 568-573.

[19] A.Saccone, S.Delfino, D.Macciò and R.Ferro. Magnesium-rare earth phase diagrams: experimental investigation of the Ho-Mg system, *J. Phase Equilibria*, 14 (1993), 280-287.

[20] A.Saccone, S.Delfino, D.Macciò and R.Ferro. Phase equilibria in the binary rare earth alloys: the erbium-magnesium system, *Metall. Trans.*, 23A (1992), 1005-1012.

[21] A.Saccone, D.Maccio', S.Delfino and R.Ferro. The interpolated Tm-Mg phase diagram, *J.Alloys and Compounds*, 220 (1995), 161-166.

[22] A.Pisch, R.Schmid-Fetzer, G,Cacciamani, P.Riani, A.Saccone, R.Ferro Mg-rich phase equilibria and thermodynamic assessment of the Mg-Sc system, *Z.Metallkde*, 89 (1998), 474-477.

[23] K.A.Gschneidner, Jr. On the interrelationships of the physical properties of lanthanide compounds: the melting point, heat of formation and lattice parameter(s), *J.Less-Common Metals*, 17 (1969), 1-12.

[24] K.A.Gschneidner, Jr. and O.D.McMasters. Systematik der Seltenerdmetall-Blei Legierungen, *Monatsch. Chem.*, 102 (1971), 1499-1515.

[25] S.P.Yatsenko, A.A.Semiannikov, B.G.Semenov and K.A.Chuntonov. Phase diagrams of rare earth metals with gallium, *J.Less-Common Metals*, 64 (1979), 185-199.

[26] S.Delfino, A.Saccone and R.Ferro. Alloying behaviour of indium with rare earths, *J.Less-Common Metals*, 102 (1984), 289-310.

[27] P.R.Subramanian and D.E.Laughlin. The copper-rare earth systems, *Bull. Alloy Phase Diagrams*, 9 (1988), 316-321.

[28] R.Ferro, S.Delfino, G.Borzone, A.Saccone and G.Cacciamani. Contribution to the evaluation of rare earth alloy systems. *J.Phase Equilibria*, 14 (1993), 273-279.

[29] G.Cacciamani, A.Saccone, G.Borzone, S.Delfino and R.Ferro. Computer coupling of thermodynamics and phase diagrams: gadolinium-magnesium system as an example, *Thermochimica Acta*, 199 (1992), 17-24.

[30] Q.Ran, H.L.Lukas, G.Effenberg and G.Petzow.Thermodynamic optimisation of the Mg-Y system, *Calphad*, 12 (1988), 375-381.

[31] J.E.Pahlman and J.F.Smith. Thermodynamics of formation of compounds in the Ce-Mg, Nd-Mg, Gd-Mg, Dy-Mg, Er-Mg and Lu-Mg binary systems in the temperature range 650° to 930° K, *Metall. Trans.*, 3 (1972), 2423-2432.

[32] J.F.Smith, D.M.Bailey, D.B.Novotny and J.E.Davison. Thermodynamics of formation of yttrium-magnesium intermediate phases, *Acta Metall.*, 13 (1965) 889-895,

[33] L.Kaufman and H.Nesor. Theoretical approaches to the determination of phase diagrams, *Ann. Rev. Mater. Sci.*, 3 (1973), 1-15.

[34] I.Ansara, C.Bernard, L.Kaufman and P.Spencer.A comparison of calculated phase equilibria in selected ternary alloy systems using thermodynamic values derived from different models, *Calphad*, 2 (1978), 1-15.

[35] H.L.Lukas, E.-Th. Henig and B.Zimmermann. Optimisation of phase diagrams by a least squares method using simultaneously different types of data, *Calphad* 1 (1977), 225-236.

[36] H.L.Lukas, J.Weiss and E.-Th. Henig. Strategies for the calculation of phase diagrams, *Calphad* 6 (1982), 229-251.

[37] B.Sundman, B.Jansson and J.-O.Andersson. The Thermo Calc databank system, *Calphad*, 9 (1985), 153-190.

[38] L.L.Rokhlin. *Magnesium alloys containing rare earth metals*, Nauka Ed.,(in russian) Moskow, 1980.

[39] A.A.Nayeb-Hashemi and J.B.Clark. Magnesium-Yttrium. In A. A.Nayeb-Hashemi and J.B.Clark (Eds.) *Phase Diagrams of Binary Magnesium Alloys*, ASM International, 1988, pp. 344-349.

[40] L.L.Rokhlin. Regularities of the Mg sides of the Mg-R (magnesium-rare earth metal) phase diagrams: comments and evaluation, *J.Phase Equilibria*, 16 (1995), 504-507.

[41] G.Cacciamani, G.Borzone, A.Saccone, A.Pisch, R.Schmid-Fetzer and R.Ferro. Contributo allo studio di alcune proprietà costituzionali di leghe Al-Mg, *Proc. I Conv. Naz. Scienza e Tecnologia dei Materiali*, Lerici (La Spezia) (1997), Apr., 2-4, C49.

[42] A.Saccone, S.Delfino, D.Macciò, F.H.Hayes and R.Ferro. Phase diagram studies on the Al-Mg-Y system, *Proc. XXV Congr. Chimica Inorganica*, Alessandria, (1997), Sept.,1-4, C9.

[43] K.A.Gschneidner, Jr. From infinity to zero and back again to infinity (from mixed rare earths to ultrapure metals to pseudo-lanthanides).In G.J.McCarthy, J.J.Rhyne and H.B.Silber (Eds.), *The Rare Earths in Modern Science and Technology*, Vol.2, Plenum, New York, NY, 1980, pp. 13-23.

[44] M.Giovannini, A.Saccone, R.Marazza and R.Ferro. The isothermal section at 500°C of the Y-La-Mg system, *Metall. Trans.*, 26A (1995), 5-10.

[45] H.Flandorfer, M.Giovannini, A.Saccone, P.Rogl and R.Ferro. The Ce-Y-Mg system, *Metall. Trans.*, 28A (1997), 265-276.

[46] M.Giovannini, A.Saccone and R.Ferro. Phase relationships at 500°C in the Y-Pr-Mg system, *J.Alloys and Compounds*, 220 (1995), 167-173.

[47] M.Giovannini, A.Saccone, H.Flandorfer, P.Rogl and R.Ferro. On the systematics of phase equilibria in complex magnesium-rare earth systems: Gd-Y-Mg system, *Z.Metallkde.*, 88 (1997), 372-378.

[48] A.Inoue. Amorphous, quasicrystalline and nanocrystalline alloys in Al- and Mg-based systems. In K.A.Gschneidner, Jr. and L.Eyring (Eds.), *Handbook on the Physics and Chemistry of Rare Earths*, Vol. 24, Elsevier (Amsterdam), 1997, pp. 83-219.